QC
968
.N3
1990

National Severe Storms Laboratory

Annual Report FY 1990

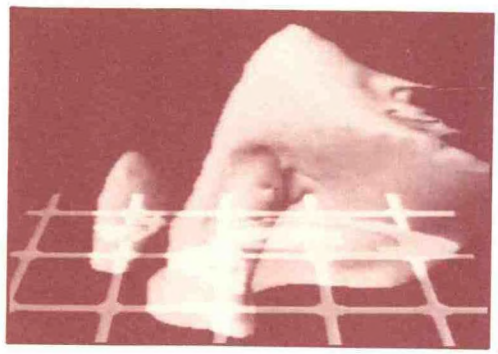

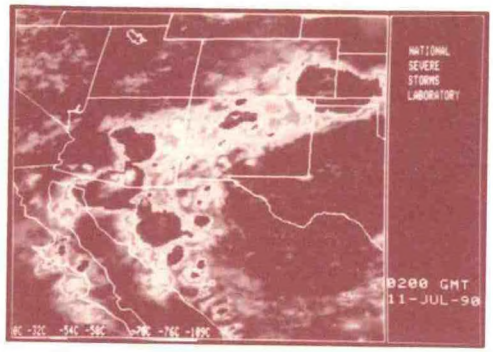

U.S. Department of Commerce

National Oceanic and Atmospheric Administration
Environmental Research Laboratories

Top Left: Computer-generated graphic of severe thunderstorm cloud outline (gray) and radar reflectivity (individual shades are shown in Figure 3). Graphic is from a videotape prepared for forecaster training in cooperation with Cray Research, Inc.

Top Right: Infrared satellite imagery view of a series of mesoscale convective systems embedded in the southwest monsoon flow from Mexico into Arizona, and northeastward into Colorado and Kansas at 0200 UTC on 11 July 1990.

Bottom: View from the NOAA P-3 aircraft of a line of convection over the Sonoran desert of Mexico during the Southwest Area Monsoon Project on 17 July 1990.

QC
968
.N3
1990

National Severe Storms Laboratory

Annual Report FY 1990

December 1990

Norman, Oklahoma

LIBRARY

AUG 9 1991

N.O.A.A.
U.S. Dept. of Commerce

U.S. Department of Commerce

National Oceanic and Atmospheric Administration
Environmental Research Laboratories

CONTENTS

THE NSSL MISSION

The National Severe Storms Laboratory conducts a broad program of research to develop basic understanding of severe weather phenomena, including large-scale and mesoscale environments that evolve and interact to produce intense storms. The focus is on observational and theoretical studies of hazardous, middle-latitude weather phenomena such as tornadoes, hailstorms, lightning, windstorms, floods, and blizzards. NSSL often participates in research field programs, usually in coordination with other ERL components and external agencies. Sophisticated numerical models are frequently employed as research tools. The Laboratory's research projects provide sound scientific foundations upon which improvements to NOAA's weather and climate forecasting services can be built. The Laboratory works directly with the National Weather Service to improve capabilities to detect, forecast, and warn of hazardous weather events.

FOREWORD

The National Severe Storms Laboratory (NSSL) develops means for improving weather forecasting through studies of storm processes, numerical and conceptual modeling of storm phenomena, and applications of new remote-sensing technologies in the severe weather environment. The work at NSSL, probably the most substantial precursor of the major national initiative NEXRAD, continues to support that program, and major efforts in the Laboratory are directed toward scientific support of the National Weather Service Modernization.

The Mesoscale Research Division (MRD) of NSSL, situated in Boulder, Colorado, gives heavy emphasis to studies of mesoscale convective systems based on data gathered during field programs. Integration of observations from the P-3 aircraft, satellites, ground-based radars, and lightning strike networks contributes substantially to MRD research.

Through numerous relationships with other government agencies and universities, NSSL constitutes a resource for severe-storm data examined by researchers around the country and overseas. NSSL participates in many research projects outside Oklahoma; for example, during FY 1990, NSSL staff participated in the Terminal Doppler Weather Radar field project at Orlando, Florida, and worked with the National Weather Service Western Region, the Salt River Project, and many other agencies, including several in Mexico, to gather P-3, radar, and mobile CLASS sounding data during the summertime monsoon over Arizona and northwest Mexico.

During coming years, increased emphasis will be given to the expansion of research to include larger scales of meteorological phenomena, and to the incorporation of modern research workstations, wind profilers, and digital satellite data into both case study analyses and the development of conceptual and numerical models. The Laboratory is a principal participant in the National Science Foundation's Science and Technology Center, CAPS (Center for Analysis and Prediction of Storms), at the University of Oklahoma. The Center's work focuses on development of new-generation numerical forecast models capable of explicit prediction of individual severe storms and storm systems.

APPLICATIONS AND FORECASTING

NEXRAD Radar

Data collected during the Interim Operational Test and Evaluation (IOT&E II), held from March to September 1989, have been examined to determine their quality and to find the best methods for their effective use in warnings and forecasts. These data were collected by the NEXRAD radar, now called by its operational designation of WSR-88D. Mesocyclones, precursors to tornadoes, were detected throughout the quantitative range of the radar (230 km), indicating the capability of these radars to assist in warnings over broad areas (Figure 1). This result should allay fears that the radars would detect mesocyclones only at relatively close ranges.

A few problems in data quality adversely affected radar algorithm performance. Algorithm performance, however, was judged acceptable in many cases. A thorough review of the algorithms revealed that certain enhancements would improve skill scores. Therefore, the National Severe Storms Laboratory (NSSL) has developed experimental versions of several algorithms to test potential improvements. Based on IOT&E data and NSSL research Doppler data collected in recent years, it appears that improvements of 20 to 50% can be achieved for storm identification and tracking, mesocyclone detection, and hail detection algorithms. In cooperation with the Atlantic Oceanographic and Meteorological Laboratory (AOML), work continues on the development of a tropical cyclone detection and tracking algorithm. Further independent testing of all the new algorithms awaits collection of new data sets in 1991.

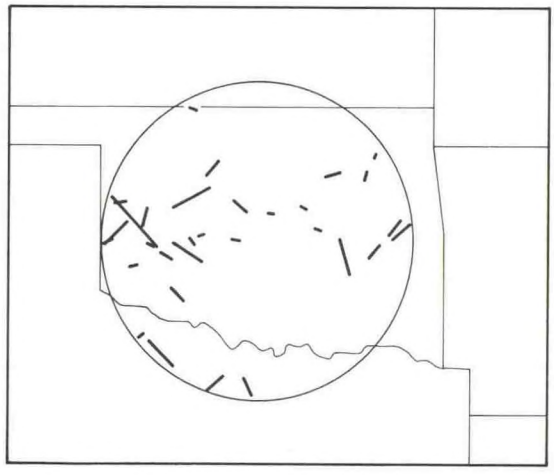

Figure 1. Tracks of mesocyclones detected by the NEXRAD Doppler during a spring and summer test in 1989. Range circle is 230 km from Norman, Oklahoma, and indicates maximum range for processing of Doppler information.

Training

NSSL continued to support the NEXRAD Training Branch, a part of the Norman Operational Support Facility (OSF). Some materials were developed and many others were reviewed as the Operations Training Course was created and the first classes were taught. In association with the National Weather Service (NWS), remote training modules on convection and radar were developed. As part of that development, graphics from an elaborate three-dimensional cloud model (facilities provided by Cray Research, Inc.) were used to illustrate the relationships between reflectivity seen by radar and the overall cloud structure of severe thunderstorms (Figure 2). NSSL assisted the U.S. Air Force's Air Weather Service (AWS) by preparing a series of videotapes on identifying hazardous phenomena using Doppler radar. In addition, seminars and workshops on mesoscale and radar meteorology were presented at several NWS offices and at other locations.

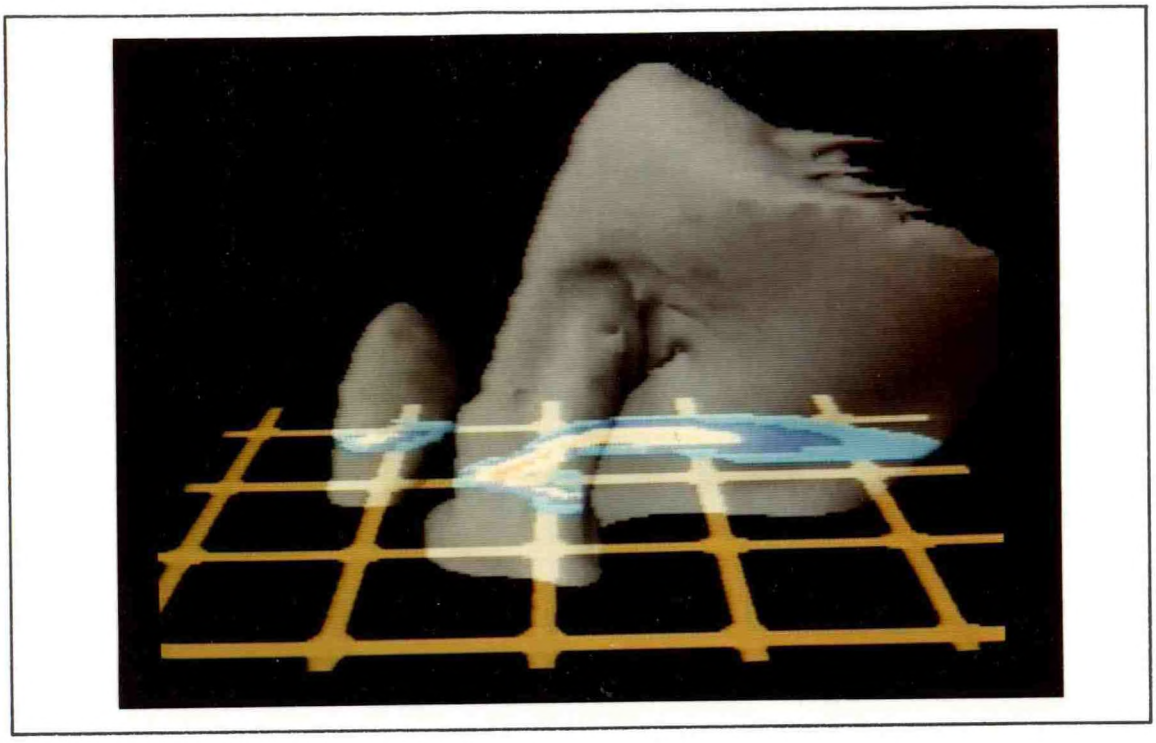

Figure 2. The outer surface of a severe thunderstorm cloud is outlined in gray. The intensity of precipitation is shown in a similar manner to radar reflectivity at lower levels by light blue for the weakest precipitation, then dark blue, white, and yellow for stronger rates. This computer-generated graphic is from a videotape prepared for forecaster training, in cooperation with Cray Research, Inc.

Profiler Applications

In anticipation of the installation of the Profiler Demonstration Network, testing and evaluation of applications for profiler data have begun, using 1985 PRE-STORM data. Kinematic parameters were computed from profiler winds and quantitatively compared to values computed from a dense network of rawinsonde observations. Both the generalized and the geostrophic thermal wind equations were used to retrieve horizontal gradients of virtual temperature. Results (Figure 3) indicate that estimates from the generalized thermal wind equation compare favorably with those computed from rawinsonde temperature measurements. Accurate temperature gradients can be used to infer changes in atmospheric stability, which is important for convective storm forecasting.

Melbourne NWS-Kennedy Space Center Forecasting Interactions

Several pilot projects were initiated in 1990 to improve forecaster awareness of the convective climatology in central Florida with the data archives at NSSL's Mesoscale Research Division (MRD) in Boulder. These projects involved personnel at NWS forecast offices in central Florida, especially the new Melbourne WSO that is targeted to receive the second WSR-88D, as well as AWS forecasters at the Kennedy Space Center (KSC).

The NSSL/MRD satellite archive was used to examine convective development across the Florida peninsula to show the magnitude of the potential for strong deep convection during southwest flow (Figure 4).

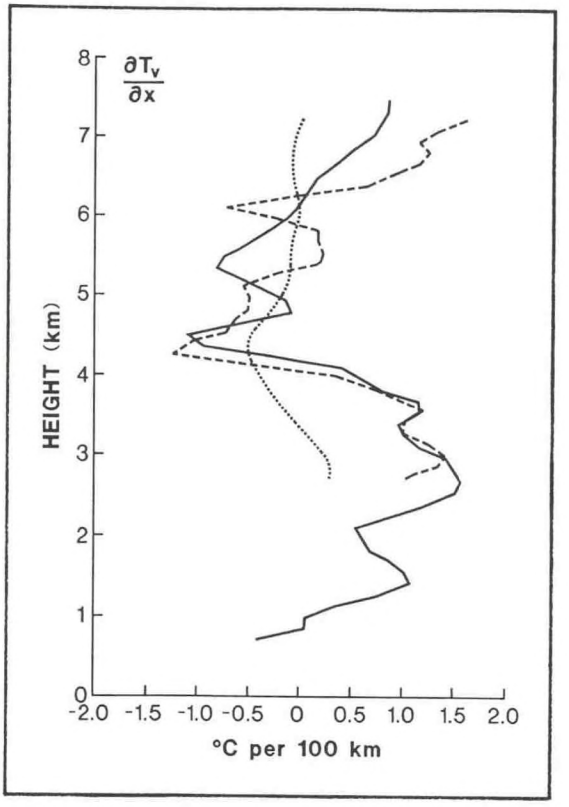

Figure 3. West-east gradients of virtual temperature at 0000 UTC 13 May 1985. Gradients calculated from Woodward and Enid rawinsondes constitute the solid curve. Gradients retrieved from profiler winds using generalized (geostrophic) thermal wind equation constitute the dashed (dotted) curve.

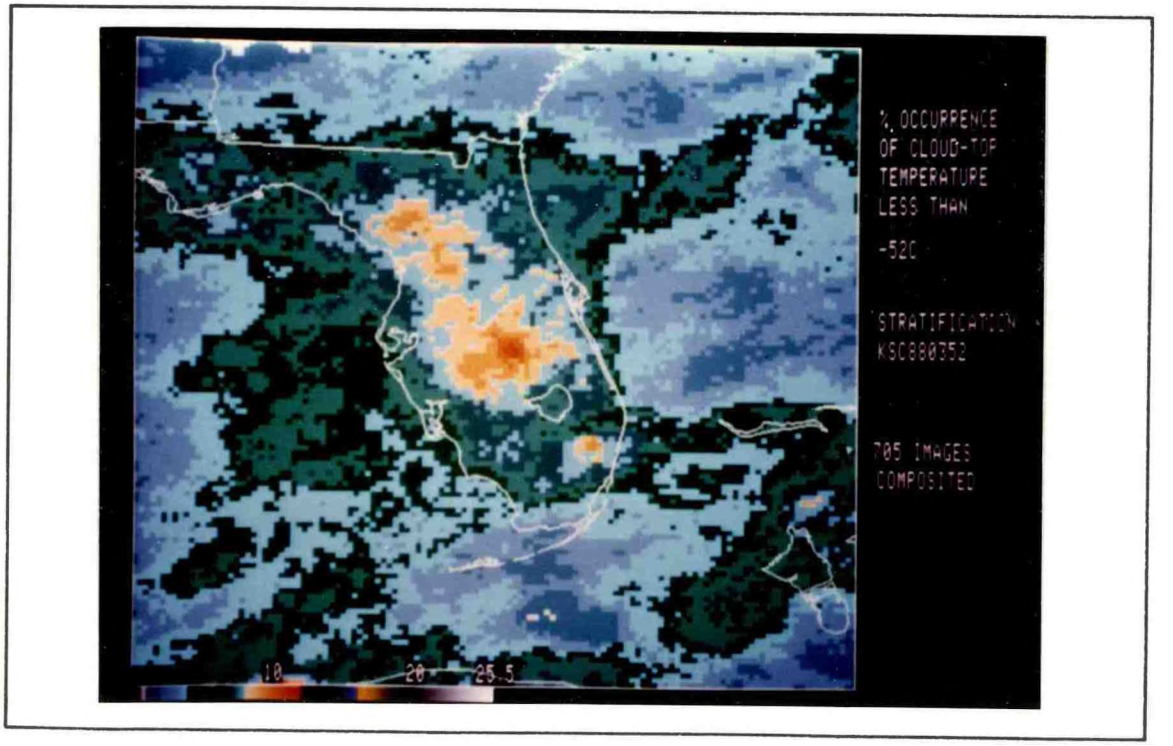

Figure 4. Percent occurrence of cloud-top infrared temperatures below -52°C for low-level southwest flow during the convective season of 1988. Note maximum frequency north of Lake Okeechobee.

Future plans include using the satellite archive for 1985 through 1990 to develop a full satellite convective climatology sorted according to synoptic winds and moisture regimes.

Hourly surface thunderstorm reports from KSC were provided by staff at NASA's Marshall Space Flight Center. This information was merged with 21 years of Cape Canaveral rawinsonde data obtained from the NSSL/MRD upper-air archive and NWS. Diagrams of the percentage frequency of thunderstorms were made, based on the synoptic winds and moisture. Figure 5 shows the high probability of storms in June and July between 1400 and 1800 EST during southwest low-level flow and high relative humidity in the middle levels from 700 to 500 mb.

Cloud-to-ground lightning data from the three direction finder (DF) network at KSC since 1983 are being reanalyzed using the Passi/López optimization scheme. As each year of this archive is corrected, a gridded set of flash information is calculated to fill hourly 10 x 10-km bins in a spherical earth coordinate system. Plans for this archive include developing a long-term central Florida lightning climatology based on wind, moisture, and stability regimes; studying interannual variability and land/ocean contrasts; and studying relationships to severe weather in the region.

Long-Lived Derecho Environment

In collaboration with staff from the National Severe Storms Forecast Center (NSSFC) in Kansas City, several NSSL scientists have studied the character of derecho environments that produce unusually long-lived and damaging events. Forecasting severe thunderstorm development during the late spring and summer months can be particularly challenging to the operational meteorologist.

Data for the study confirm that low-level warm advection is typically associated with derecho genesis. Examination of composite charts indicates a significant

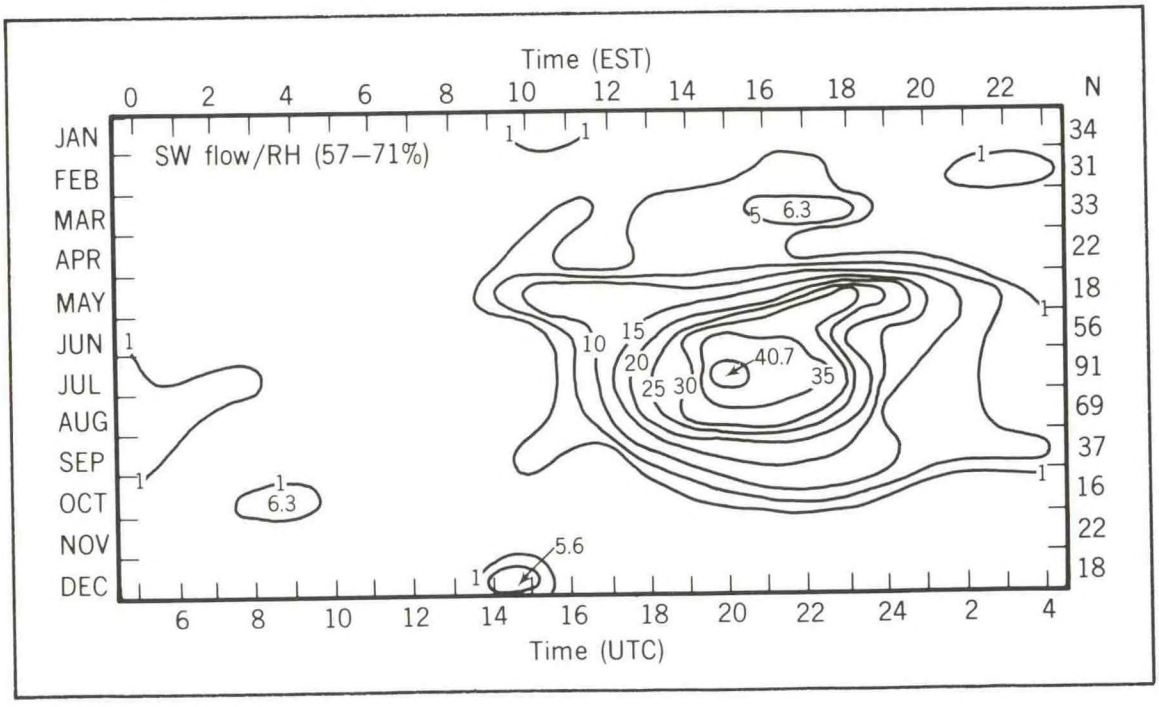

Figure 5. Probability of thunderstorms on the Kennedy Space Center as a function of month and time of day.

veering of winds with height near the initiation region. However, as the long-lived derecho-producing convective systems move eastward along the low-level thermal gradient, the low-level flow becomes increasingly parallel to the higher-level winds and the low-level jet weakens or disappears (Figure 6, top). Although long-lived derechos progressively move into a classically more unfavorable wind pattern, the convective systems intensify and accelerate as they approach the midpoint. The most damaging winds usually occur as the systems encounter the most unstable air along their path. It appears that once a long-lived derecho commences, the associated gust front dominates as a lifting mechanism as the upward vertical motion resulting from low-level warm advection decreases.

The composite derecho pattern from this study is contrasted with a more typical severe storm pattern (Figure 6, bottom). The derecho composite may help operational forecasters identify situations that support the development of a long-lived derecho.

Terminal Doppler Weather Radar (TDWR)

The Federal Aviation Administration (FAA) is developing a terminal-area Doppler radar that will be deployed near the nation's largest airports. This system will detect and forecast the arrival of wind-shear events automatically up to 20 minutes in advance. During the past year, NSSL continued to develop and enhance two algorithms to be used in TDWR. A gust front detection and prediction algorithm has been under development since the mid-1980s, and a tornadic vortex signature (TVS) algorithm is in its second year of construction.

NSSL participated in the FAA's TDWR test and evaluation in the vicinity of Orlando, Florida, during the summer of 1990. The algorithm for gust front detection and wind shift prediction ran in real time on the Massachusetts Institute of Technology (MIT)/Lincoln Laboratories Doppler radar near Orlando, and the algorithm output was displayed in the air traffic control tower.

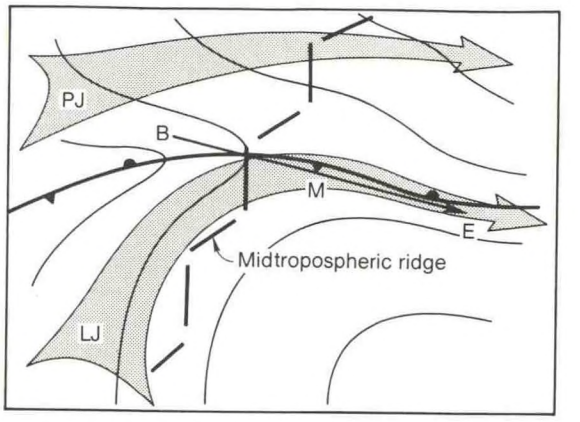

Figure 6 (top). Idealized sketch of a composite large-scale pattern associated with long-lived derechos. Thin lines denote sea-level isobars around a low-pressure center with cold and warm fronts. Broad arrows represent low-level jetstream (LJ) and polar jet (PJ) in upper troposphere. The damage axis B-E is 1400 km (750 nautical miles) long.

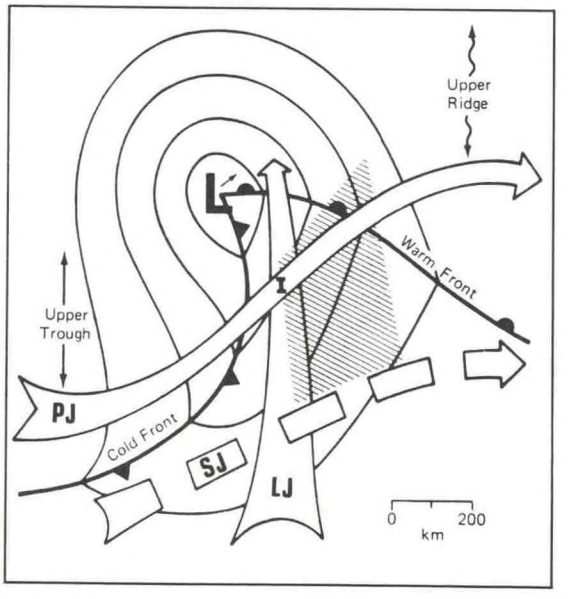

Figure 6 (bottom). Sketch similar to Figure 6 (top) for the middle-latitude, synoptic-scale situation especially favorable for development of severe thunderstorms. Subtropical jet (SJ) is shown for a somewhat higher level in the upper troposphere (after Barnes and Newton in **Thunderstorm Morphology and Dynamics**, *E. Kessler, Editor, 1985).*

Controllers had good success in using the displays to warn for and plan around wind-shear hazards. One NSSL mobile laboratory (with M-CLASS) was driven to Orlando and took more than 50 soundings during the test. The M-CLASS system in the mobile laboratory is the Mobile Cross-chain LORAN (Long-Range Aid to Navigation) Atmospheric Sounding System. Together with the radar data, these soundings will be used to study the initiation of thunderstorms in subtropical environments and to examine the origination of gust fronts and microbursts.

The NSSL gust-front algorithm has been upgraded to detect approximately 88% of all strong gust fronts, and forecast their future locations up to 20 minutes in advance. Real-time evaluations in 1990 were carried out in the southern United States at Orlando and on the High Plains at Denver. In addition, an advanced gust front algorithm (AGFA) has been developed during the past year. The AGFA incorporates the detection of reflectivity thin lines and azimuthal shear, along with the previous gust-front algorithm's detection of radial convergence, to give a more robust output of gust front location.

A computer algorithm using single-Doppler data to detect TVSs was developed for the TDWR program. A TVS is a very strong indication of the formation of a tornado. Algorithm output is generated every 2.5 minutes and is divided into two categories: TVS and PTVS (potential TVS). A PTVS indicates a signature aloft, whereas a TVS indicates a signature aloft and near the surface.

During the summer of 1991, NSSL scientists plan to participate in another TDWR test in Florida, perhaps using a mobile laboratory to release additional soundings. The TDWR project goals for NSSL in 1991 are to further test the AGFA and TVS algorithms in real-time settings in Florida, Oklahoma, and Colorado, then to transfer code for both algorithms to the TDWR contractor.

Doppler Radar Support for NWS

Because output from NEXRAD radars was unavailable during the warm season of 1990, NSSL used its Norman research Doppler radar to support warning operations at the Oklahoma City Area NWS Forecast Office (NWSFO) located in Norman. Many hours were spent in operating the radar, presenting displays in the NWSFO, and consulting with forecasters about signatures that appeared on the displays. On 13 March 1990, 10 strong tornadoes produced significant damage and some injuries in Oklahoma, but no fatalities. On 15 May 1990, a very strong tornado moved through Stillwater, Oklahoma, producing over $6 million in damage, injuries, and one fatality. NWS provided an excellent early warning, with lead times of 15 to 20 minutes, that is credited with minimizing the casualty and fatality toll for the passage of such a strong tornado through a large town. The warning was based on the detection of an intense mesocyclone signature, seen on displays of Norman Doppler velocities (Figure 7). The public also received five timely updates of tornado development and precise location as it moved toward, through, and past the town, along a 12-mile path.

Mesoscale Weather Forecasts

The fourth in a series of forecasting experiments was carried out during the spring and fall, in cooperation with the NWSFO in Norman. These experiments were designed to explore the feasibility of forecasting various aspects of convective storms. Emphasis has also been focused on interactions between the project forecasters and the operational forecaster team on duty at the office.

Results of the experiments are still being analyzed, but several issues about the experimental forecasts have become clear over the 4 years of the project to date.

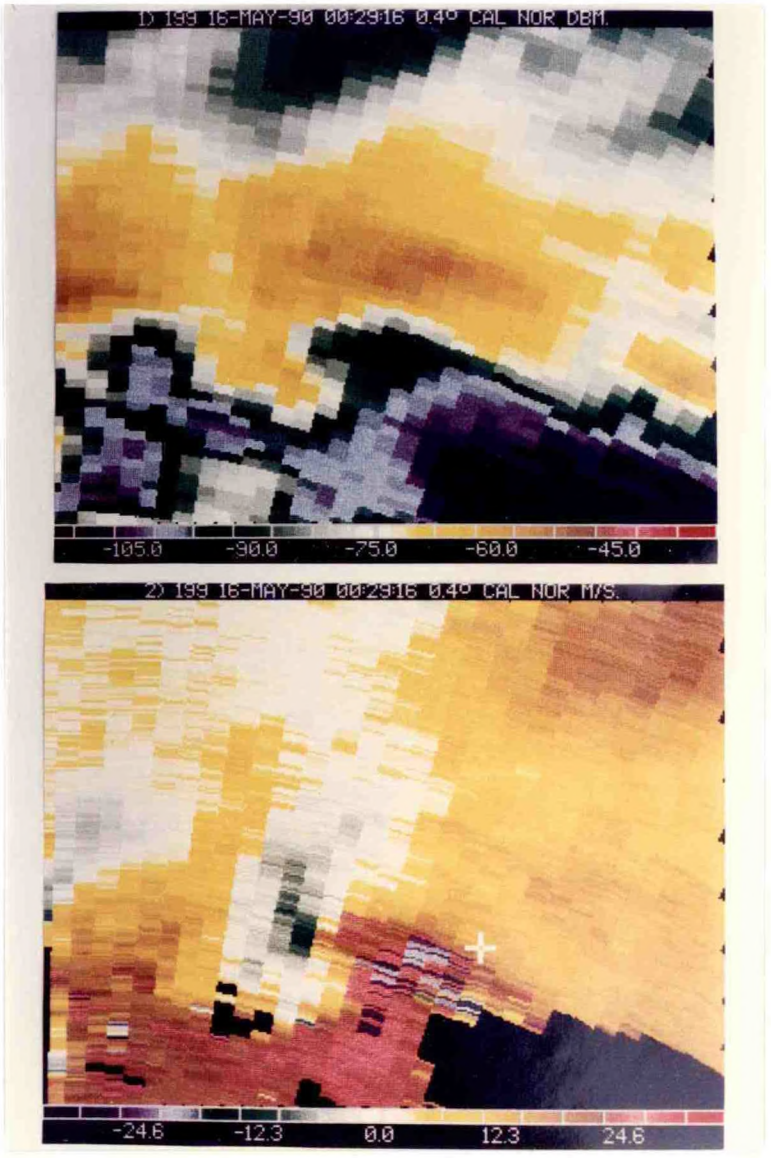

Figure 7. Norman Doppler reflectivity (top) and velocity (bottom) at 0.4° elevation for 1829 CST on 15 May 1990. Reflectivity scale is dBm and velocity is m s^{-1}. Cursor in bottom panel is at Stillwater, Oklahoma, where a tornado struck between 1845 and 1850 CST.

- Forecast products must include at least some rigorously verifiable forecast elements. This has not always been as simple to do as it would appear, because often problems do not surface until after the experiment has begun.
- A verification scheme must be well matched to the problem at hand. Verification techniques for rare events are not as well developed as for common events, so some new verification schemes have had to be developed.
- It is critical to follow verification with a careful meteorological analysis of the reasons for both successes and failures detected during the verification process. This issue is both knowledge intensive and time consuming.

If forecast experiments are to improve operational forecasting, these three issues are very important. Concepts developed in this continuing program of forecasting experiments should enhance the STORM Project's Experimental Forecast Center concept as well as provide important feedback on the modernization and restructuring program of NWS.

One of the convective forecasts attempted in 1988 was to specify the convective mode and extent of MCSs 9 hours in advance by forecasting the outlines of cold cloud tops and verifying the forecasts with infrared satellite images (see Figure 8 for an example). Although the skill scores were determined to be no more than 35%, the results are useful because they benchmark current skill with available inputs. They also can be compared to future forecasts based on additional mesoscale observational tools such as NEXRAD, profilers, next-generation satellites, and mesoscale models.

A new parameter, storm-relative helicity, has been developed as a predictor of mesocyclones and tornadoes. It was tested for the first time during the spring of 1990 as part of the mesoscale convective forecast experiments with the Norman NWSFO. Input winds were obtained from operational rawinsonde releases, special NSSL M-CLASS soundings, and operational numerical model output. Mesocyclone forecasts in 1990 were more successful than those issued during the past three springs (Figure 9). This result suggests that storm-relative helicity is useful in forecasting and important in raising forecaster awareness of the role of low-level wind shear in mesocyclone development.

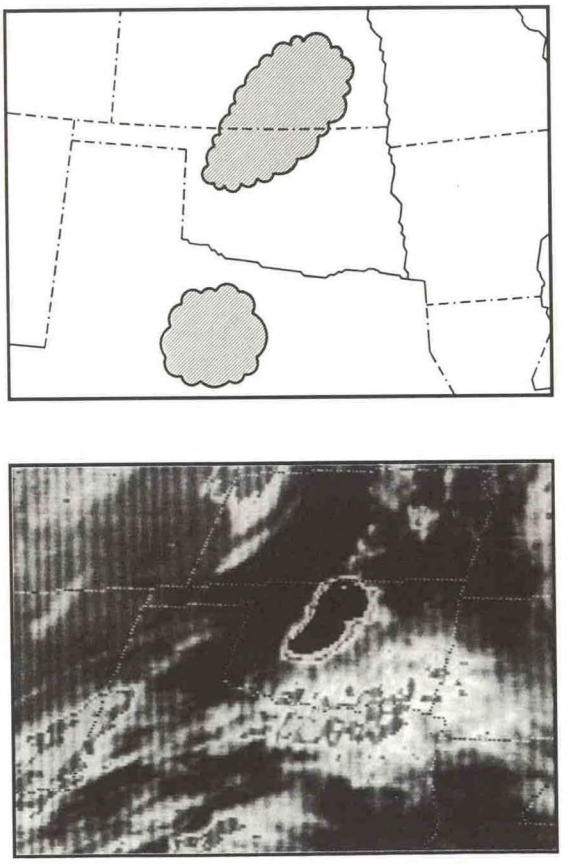

Figure 8. Nine-hour forecast of satellite infrared cold-cloud outline (top) and verifying infrared image (bottom) at 0600 UTC 7 May 1988. The northern MCS is well forecast, but the southern system is not. Remnant clouds on the satellite image show the remains of a weaker southern system, which had dissipated by forecast verification time.

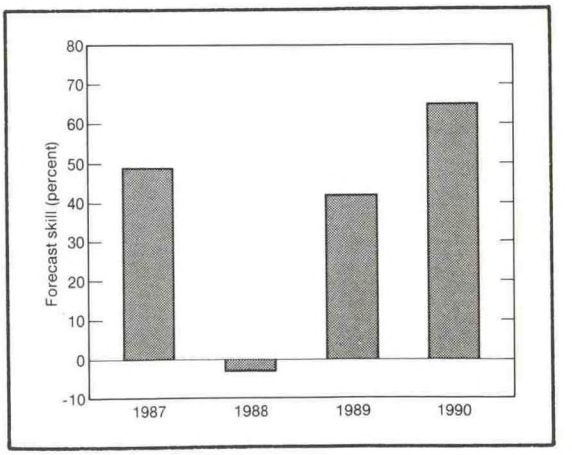

Figure 9. Skill scores of spring mesocyclone forecasts for 1987-1990. A score of 100 would be perfect skill and scores near 0 are low skill.

Microburst Handbook

The publication *Microbursts: A Handbook for Visual Identification* was printed in color for a third time during the year, bringing the total printed to more than 14,000 copies. This second edition adds English-unit equivalents to all parameters, to be more directly applicable to aviation interests that employ these values. A poster edition of the booklet is near completion for printing.

A new publication, *Severe Weather: A Handbook for Visual Identification,* will be prepared in FY 1991 to assist the general public in identifying many different types of severe weather that require immediate action, such as flash floods, funnels, and gust fronts. The publication will emphasize their visual appearance under conditions that are less than ideal or not typical.

Four-Dimensional Data Assimilation

NSSL continues to play a key role in assimilating data for mesoscale and synoptic-scale modeling with CAPS, the Center for the Analysis and Prediction of Storms at the University of Oklahoma. Four areas are under investigation:

- Use of parallel processing machines to analyze winds from Doppler radar and satellite, in conjunction with the University of Oklahoma Computer Science Department.
- Investigation of optimal initial states for nonlinear dry convection models, in conjunction with the University of Oklahoma School of Meteorology.
- Study of variational data assimilation with frontal models, in conjunction with the Pennsylvania State University.
- Study of mathematical foundations of adjoint data assimilations with nonlinear models, in conjunction with the University of Oklahoma Department of Mathematics.

Warm-Cloud Microphysical Parameterization

Work is under way in cooperation with the Cooperative Institute for Mesoscale Meteorological Studies (CIMMS) to evaluate and improve the parameterization of warm-rain microphysical processes. The main tool is the three-dimensional detailed microphysical cloud model maintained by CIMMS. This model contains detailed physics for the complete warm-rain formation process. Running this model with detailed microphysics and parameterization allows a direct evaluation of how well bulk parameterization can simulate the detailed microphysics. The model further functions as an invaluable development tool for making improvements to the parameterization, because the evolution of bulk variables can be directly followed within the detailed model run data set. Thus far, the detailed condensation process can be very accurately represented using a simple modification of a widely used bulk condensation method. Remarkable agreement has also been found (Figure 10) between the detailed and bulk-parameterized coagulation rates. The bulk method evaluated for Figure 10 was originally developed by NSSL in 1969, and is still in widespread use. The slope of the numerical data in Figure 10 is not consistent for different model runs. Nevertheless, these results suggest that current work to modify the 1969 NSSL scheme will be able to accurately represent the detailed coagulation process.

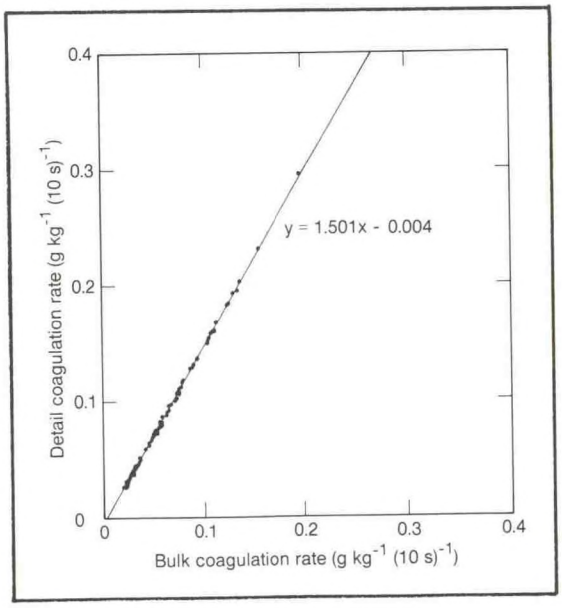

Figure 10. Scatter plot comparing bulk versus detailed representation of the coagulation rate at 1800 seconds into a warm-cloud model run. Plotted points are from locations throughout the three-dimensional cloud where the bulk rate exceeded 0.02 g kg^{-1} 10 s^{-1}.

Penn State-NCAR Mesoscale Model Applications

The Pennsylvania State University/National Center for Atmospheric Research (NCAR) mesoscale model is being used in collaboration with scientists at the university to simulate the development and evolution of numerous mesoscale convective systems (MCSs) on 12 May 1982 that produced flash floods in Oklahoma and Texas. Analyses of upper-air data show that large-scale forcing was very weak, so the evolution of the atmosphere over the southern Plains apparently was controlled by mesoscale processes and their interactions. In this type of situation, the physics of the model are crucial to the correct evolution of the events. Early model results suggest that decision criteria for where and when parameterized, deep convection is initiated by the model must be considered carefully. In addition, the appropriate specification and placement of subsynoptic convective outflows in the model's initial conditions are required to produce a simulation that approaches reality. It is not yet clear whether the model can simulate accurately the initiation and evolution of each individual convective system. However, simulation of the general evolution of atmospheric structure appears to be within the capability of the model.

Deduction of Storm Reference Frame Motions

Many applications require a good, objective estimate of storm motion. One can define storm motion as the velocity of a reference frame in which time changes are minimized. Applying dynamic retrieval to Doppler velocity data for a series of assumed reference frame motions for a given storm can give an "optimal" storm motion; thus far these motions have been determined for four different severe storms. In one case, independent measurement of pressure fields by aircraft near a storm updraft was used to validate the storm motion estimate. Also, the optimal reference frame motion varies with altitude within each storm because the movement of dominant dynamic features within a storm generally varies with altitude. This concept may have implications for adjustments that are applied to data fields, such as Doppler volume scans, to produce data values at a common reference time. Figure 11 depicts this migration of optimal storm motion with altitude, and compares the resulting curve with the hodograph derived from a proximity sounding for a tornadic storm. The shapes of the two curves indicate that the environmental wind strongly influences but does not completely determine the values of optimal storm motion at each altitude.

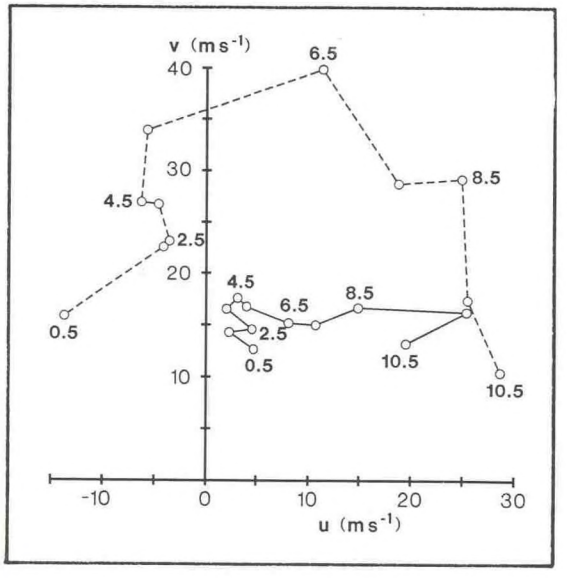

Figure 11. Optimal reference frame motion based on dynamic retrieval calculations as a function of height (solid curve) for an observed tornadic storm. Hodograph for a proximity sounding (dashed curve) taken 30 minutes before the Doppler wind analysis used in the retrieval calculations (numbers are heights in kilometers).

Thunderstorm Electrification Modeling

The Binger, Oklahoma, storm on 22 May 1981 was investigated to understand what storm conditions lead to either intracloud (IC) or cloud-to-ground (CG) flashes in tornadic storms. The study utilized observations of flashes in the mesocyclone region as well as a three-dimensional kinematic storm electrification model. In a previous study, the IC flash rate peaked during the period of greatest storm intensity, whereas the negative CG flash rate peaked about 15-20 minutes later. It is hypothesized that the intense convection in the mesocyclone region produces an elevated charge dipole conducive to IC discharges, and that the lower negative charge of the dipole subsequently descends on falling precipitation to trigger the negative CG flashes.

The hypothesis was tested by calculating the modeled charge and electric field distributions on a horizontal grid of 54 by 54 km (2-km spacing), and 19 km in the vertical (1-km spacing). The model accepted the 1909 CST multiple Doppler wind analysis

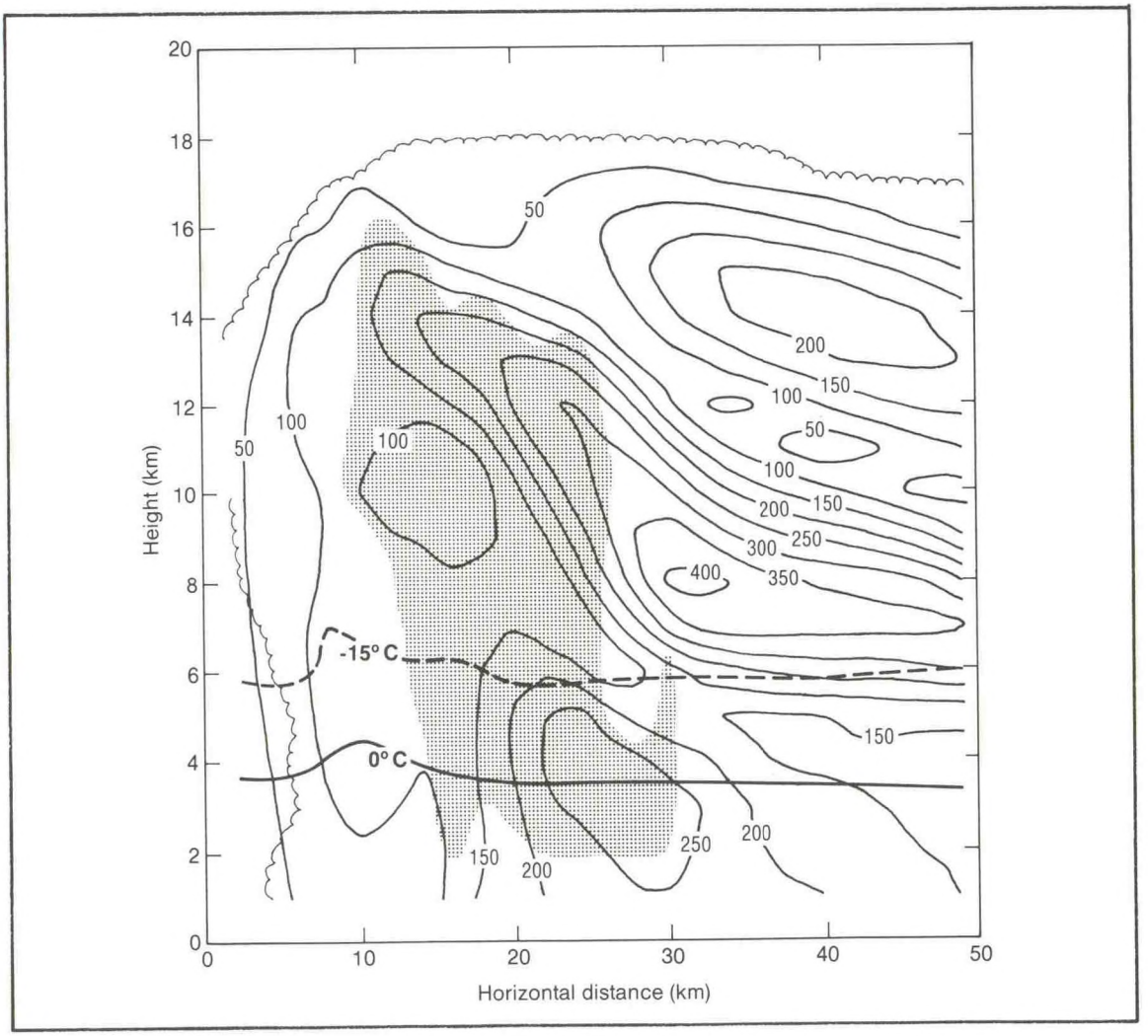

Figure 12. Magnitude of the vector electric field (kV m^{-1}) in the Binger tornadic storm as calculated by the three-dimensional cloud model. Contours are at 50 kV m^{-1} intervals. The stippled region contains updrafts of more than 5 m s^{-1}. The heavy solid line is the melting level, and the heavy dashed line is the -15°C isotherm. Scalloped line represents cloud outline.

and output fields of temperature, vapor, cloud, precipitation, charge density, and electric field. Figure 12 shows the electric field magnitude in a vertical southwest-northeast cross section. The main updraft and mesocyclone are to the left, and the anvil region (transition region) is to the right. A layer of intense fields to 300 kV m^{-1} is seen at the top of the main updraft. The strongest fields (500 kV m^{-1}) are immediately northeast of the main updraft at 7.5 km and about -25°C. This is the initiation point of repeated lightning discharges (6-12 per minute) in the model. A discharge parameterization was included to control runaway field buildup. Additionally, graupel trajectories were derived from model data. The main negative charge on graupel descended from the upper levels of the main updraft, inducing descent of the region of strong fields. Of more than 300 such trajectories starting in the main updraft, 123 reached the melting level with negative charge. Although most trajectories took between 10 and 30 minutes to descend, the average descent time of 19 minutes is consistent with the observed 15-20 minute lag of negative CG flash rate.

Data Assimilation in an MCS Model

A three-dimensional, time-dependent mesoscale kinematic model was used to study the evolution of temperature and water substance in the MCS of 7 May 1985 during PRE-STORM. The model assimilates gridded mesoscale analyses of wind and temperature with data obtained by a network of radiosondes. The outer region is constrained by the synoptic soundings, whereas the inner (mesoscale) region is constrained both by supplemental PRE-STORM soundings and by the fields from the outer region. If the radiosonde wind observations contain adequate information to retrieve temperature, vapor, cloud, and precipitation fields in the MCS anvil and associated precipitation region, then a model with comparable microphysics may be capable of assimilating the data from the Wind Profiler Network to provide initial conditions for future regional forecasts of MCSs.

The model domain extends on a horizontal grid of 700 km (25-km spacing), and 13.5 km (300-m spacing) in the vertical. The model includes resolvable-scale transportive, diffusive, and warm/cold cloud microphysical processes. Snow aggregation has recently been included, and a future version will include a parameterization of sub-grid convective processes. The model was integrated from 0000 to 1200 UTC on 7 May 1985, with 1-hourly input mesoscale objective wind analyses and time-dependent lateral boundary conditions approximated by the regional objective analysis fields. Figure 13 presents the mesoscale updraft and hydrometeor fields at 0900 UTC in a vertical north-south cross section. Ice supersaturation is present within a deep layer from the freezing level, about 3 km, to the top of the mesoscale updraft and cloud system, about 12 km. Up to 1 g kg^{-1} of snow is produced by vigorous deposition growth; this effectively excludes liquid cloud by depleting water vapor below water saturation. Besides limiting the riming growth, this result has profound implications for aircraft icing and for electrification of the associated cloud and precipitation region of the MCS. As crystals grow, they aggregate to form fewer, larger particles. Snow descends and melts below 3 km, where a fraction of the meltwater is enhanced by accretion of cloud and reaches the ground as rain. The horizontal distributions of rainfall are broadly consistent with measurements from both rain gauges and the WSR-57 radar network. The ability to model these well-known generic features of the stratiform region of an MCS with radiosonde data suggests at least marginal resolvability with Wind Profiler Network data.

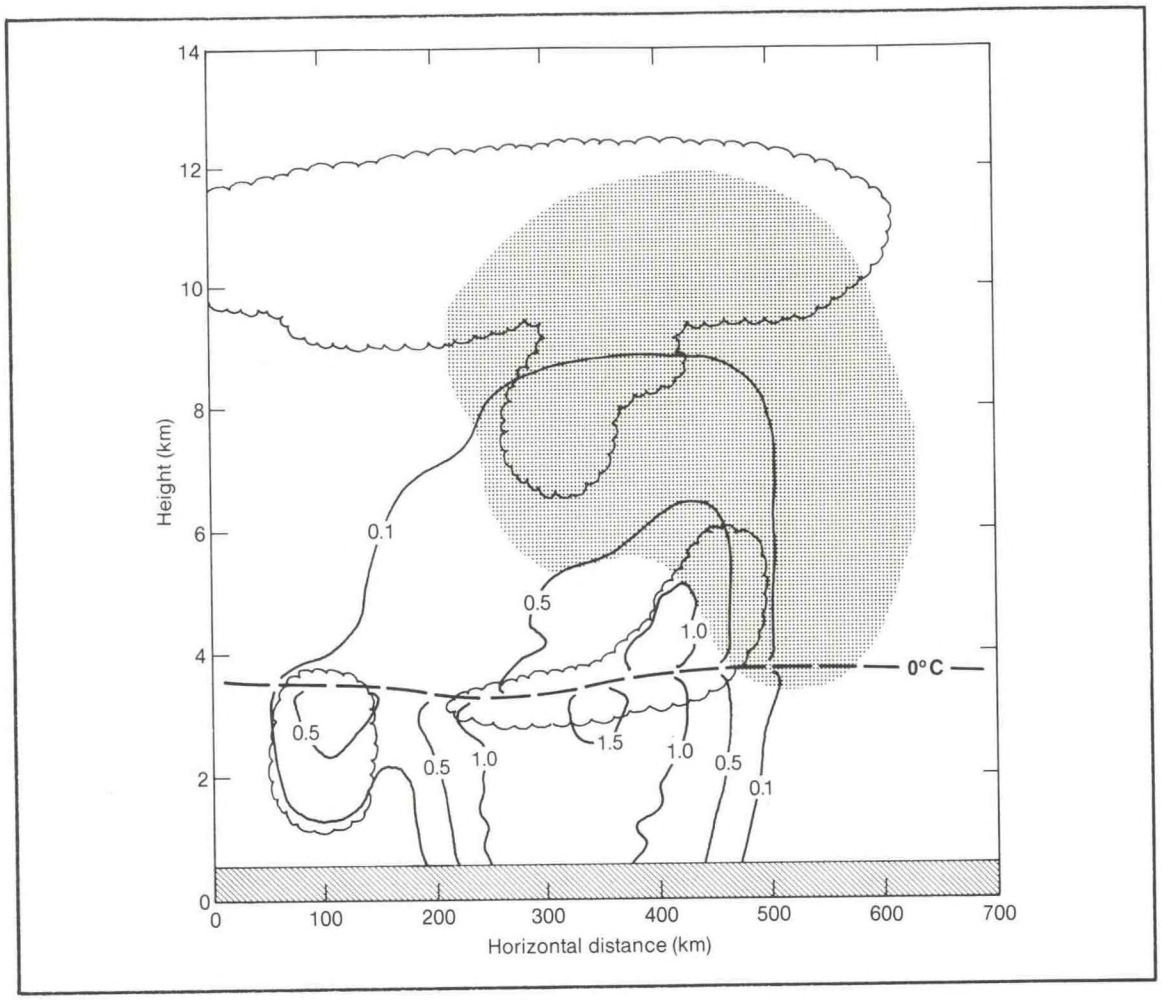

Figure 13. Output of 9-hour integration of a mesoscale kinematic model verifying at 0300 CST on 7 May 1985, in north-south vertical cross section. Shading denotes vertical velocity greater than 20 cm s^{-1}, scalloped curve outlines the cloud, and heavy dashed line is the melting level. Solid contours represent the precipitation mixing ratio in g kg^{-1}, snow (rain) above (below) the melting level (dashed line). The portion of the cross section below the terrain is hatched.

Dryline Data Analysis

Data collected in an Oklahoma dryline during the Cooperative Oklahoma P-3 Studies field program (COPS-89) were analyzed to determine the morphology of the dryline and its environment. The dryline is now hypothesized to be a zone of sharp virtual temperature contrast; the prevailing notion has been that horizontal gradients of virtual temperature at the dryline are rather weak or nonexistent. The existence of virtual temperature gradients would imply that vertical circulations develop by solenoidal forcing and that frontogenetic effects maintain a sharp moisture discontinuity.

Data were obtained from the NOAA P-3 aircraft, dropsondes, and M-CLASS releases. The P-3 executed a series of stepped traverses through the dryline on 24 May 1989 during midafternoon. Figure 14 depicts a subjective analysis of virtual potential temperature data obtained by the P-3 within the vertical section roughly normal to the surface orientation of the dryline. Substantial virtual potential temperature gradients exist at and to the east of the dryline between x values of 65 and 75 km. The data also show

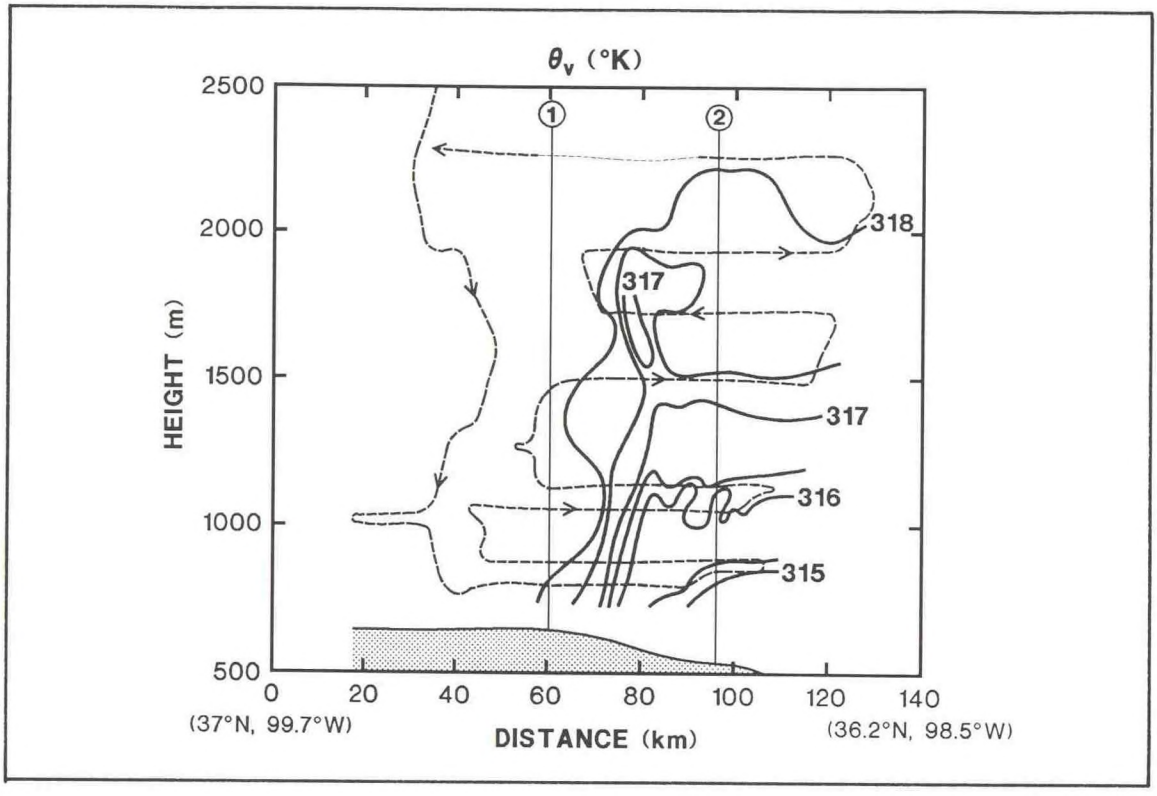

Figure 14. Subjective analysis of virtual potential temperature (°K) from NOAA P-3 aircraft measurements between 1420 and 1630 CST over northwestern Oklahoma on 24 May 1989. Contour increments are 0.5°K. Dotted line denotes the flight path projected onto the vertical cross section. The portion of the cross section below ground is stippled. Vertical lines 1 and 2 denote locations of M-CLASS soundings relative to the cross section.

that high (low) potential temperature and low (high) vapor mixing ratio are present in regions of high (low) virtual potential temperature. A deep column of moisture is present nearly over the surface dryline, and a moist layer of comparable depth is seen to the east.

Dryline Modeling

Simulations of the dryline and its environment have been initiated with the Regional Atmospheric Modeling System (RAMS) mesoscale model at Colorado State University (CSU). The goals of this cooperative study between NSSL and scientists at CSU are to identify factors that produce and maintain the dryline and are responsible for initiation of deep convection along the dryline.

A series of preliminary simulations were completed using the two-dimensional nonhydrostatic version of the model. The domain is a vertical slab oriented west-east that extends 400 km in the horizontal (2-km spacing) and 25 km in the vertical. The grid is vertically stretched from a 100-m spacing near the surface to 1000 m above 17 km. The model was initialized and verified with data collected during the COPS-89 field program on 24 May 1989. The model was integrated from 1200 UTC on 24 May to 0000 UTC on 25 May using various initial conditions for fields of soil moisture, wind, temperature, and water vapor. Figure 15 shows the output water vapor mixing ratio (g kg^{-1}) at 1800 CST in a simulation with dry soil conditions in the western portion and fairly moist soil conditions in the eastern portion. A deep, fairly dry mixed layer

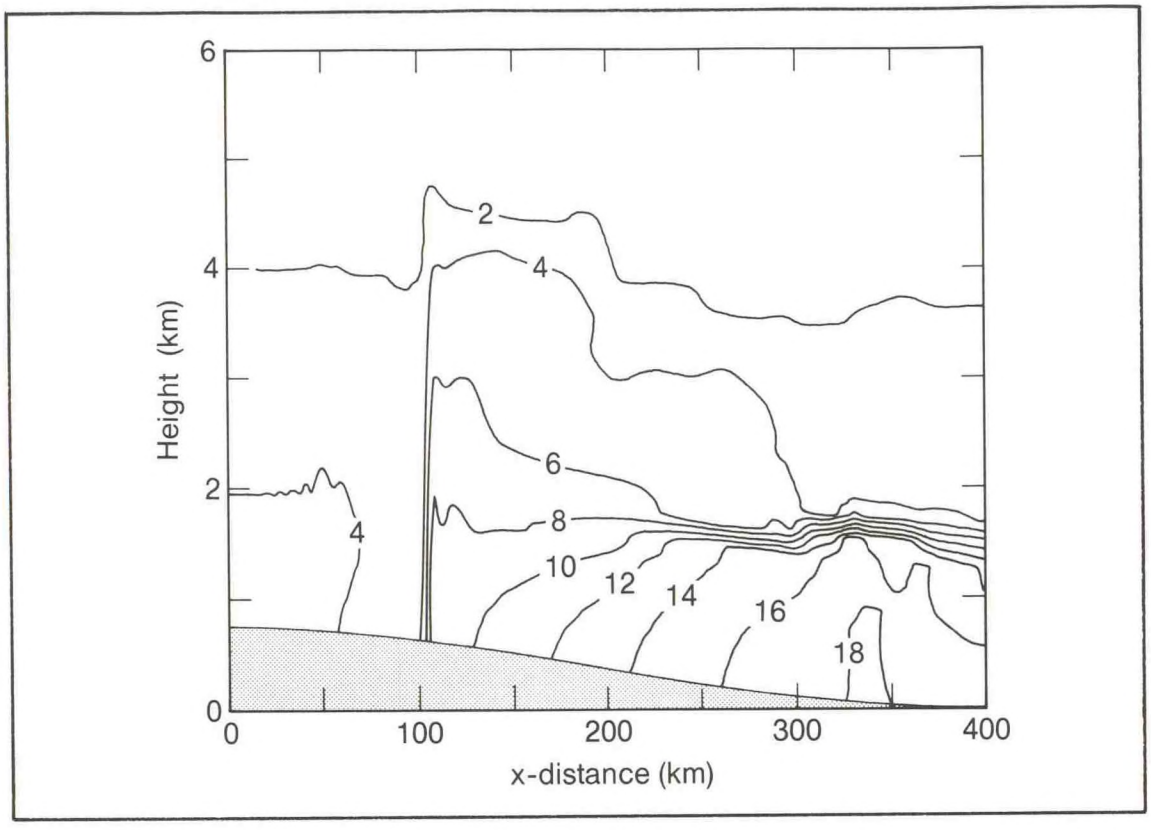

Figure 15. Simulated field of water vapor mixing ratio (g kg^{-1}) from a 12-hour integration of the CSU RAMS mesoscale model, verifying at 1800 CST on 24 May 1989. Contour intervals are 2 g kg^{-1} beginning at 2 g kg^{-1}.

(mixing ratios less than 5 g kg^{-1}) is present in the western portion of the region. Rather high mixing ratios (up to 18 g kg^{-1}) exist in a shallow layer near the surface in the eastern portion of the domain. A gradual increase of mixing ratio is seen in the boundary layer over a horizontal distance of roughly 250 km in the central portion of the domain. This feature is often referred to as the dryline in classical data analyses and some recent regional model simulations.

A simulated version of what is believed to be the true dryline is present at an x value of about 100 km. With increases of 4-6 g kg^{-1} over less than 10 km, the dryline marks the western boundary of the deeper moist layer to the east. Although the model simulates an updraft of more than 2 m s^{-1} at the dryline, the westerly winds in that region are more than 10 m s^{-1}. Hence, advective transport tends to dry out the layer above the surface position of the dryline. Vertical mixing through turbulence generated in the convective boundary layer appears to be responsible for the apparent uplift of moisture at the dryline. Horizontal advection of the lifted moisture produces a secondary moist layer overlying the higher moisture values near the surface east of the dryline. This moisture distribution is broadly consistent with the P-3 measurements, soundings, and surface measurements during COPS-89.

Convective Processes

Many numerical simulations have used the Klemp-Wilhelmson cloud model to investigate some of the basic properties of convection in the atmosphere and in models. Specifically, the forces on thunderstorm updrafts were investigated in environments with different amounts of storm-relative helicity to identify the physical processes that enhance updrafts within high-helicity environment storms in the cloud model. As a continuation of that research, testing has begun on distributions of pressure proposed in the literature in the vicinity of updrafts by using idealized numerical model simulations. Modeling of observed mesocyclone-bearing, nontornadic thunderstorms has been started. Results of initial simulations indicate that our understanding of the initiation of convection in numerical models is inadequate. Therefore, an experiment to improve that understanding with simple initialization techniques has been designed and will be carried out in 1991.

MCS Electrical Structure and Charge Generation

Data were collected in Oklahoma during COPS-89 with the NOAA P-3 aircraft, NSSL's balloon-borne electric field meters, a lightning ground strike locating system, and ground-based Doppler radars to use with other data sets to determine the electrical structure and lightning activity of MCSs. A basic understanding of physical principles and relationships among the structure, air motions, and electrical activity of these significant weather systems is being sought. Measurements of in-situ electric fields in MCSs more than tripled the amount of this type of data that are available; the first simultaneous measurements of electric field with precipitation microphysics were also collected. Observed profiles of electric fields in MCSs indicate the vertical distribution of charge is more complex than the long-accepted simple electric dipole model. Three hypotheses were developed to explain electrification of the stratiform region:

- Charge is carried from the cores into the stratiform by the internal wind,
- Charge is created and separated by colliding precipitation in the region, or
- Convective cells embedded in the region add charge.

These hypotheses will be applied in modeling efforts and are being used to plan field programs.

Satellite infrared imagery and CG lightning strikes were isolated for each of the four MCSs on 3-5 June 1985 during PRE-STORM, and time-series plots were prepared of negative CG flash rates, positive CG flash rates, the fraction of CG flashes that are positive, negative CG return strokes, positive CG return strokes, areas within temperature contours colder than -52°C, -56°C, and -60°C, and other values warmer and colder than these. Similar variables are also being examined in less detail for a large number of cases. To test the hypotheses in the models, particle size, particle charge and electric field in MCSs will be measured to determine relationships between charge on precipitation and a storm's electric field and charge distribution.

The lightning activity of a mesoscale convective complex (MCC) that originated over northeastern Colorado was studied as an early, small conglomerate of thunderstorms transformed into an MCS and later into a mature MCC. The emphasis of the study was to investigate where the CG flashes of positive and negative polarities occurred in relation to the structure of a developing cloud system. In the first 3 hours of the formation of the MCC, except for one positive flash, only negative CG flashes were produced (Figure 16). These occurred in association with distinct peak-reflectivity centers in the southwestern fringe of the growing cloud shield. During this period, the negative CG flash rate increased from zero to 360 flashes per hour. After this peak, the negative CG flash rate decreased for about 90 minutes and the positive rate increased. With time, these positives spread progressively farther downwind from the negatives and peak radar reflectivity centers into the stratiform area. During the next 90 minutes, negative CG flashes increased and the positives diminished abruptly. When this second surge peaked, the positives again increased and maintained relatively high rates as the negatives dwindled to just a few flashes. This time, however, the positives remained physically close to where the negatives had occurred before, in association with the high reflectivity fringe, with very little spread into the rest of the cloud shield. An inverse correlation between the negative and positive flashes, then, is found for this case. The two main periods of maximum positive CG flash rate coincide with minima in the negative flash production, and the two main periods of maximum negative flash rate coincide with positive minima. The positive flashes are initially found near the negatives, but as the positive rate increases, the positives are found farther from the negatives and the storm's convective area.

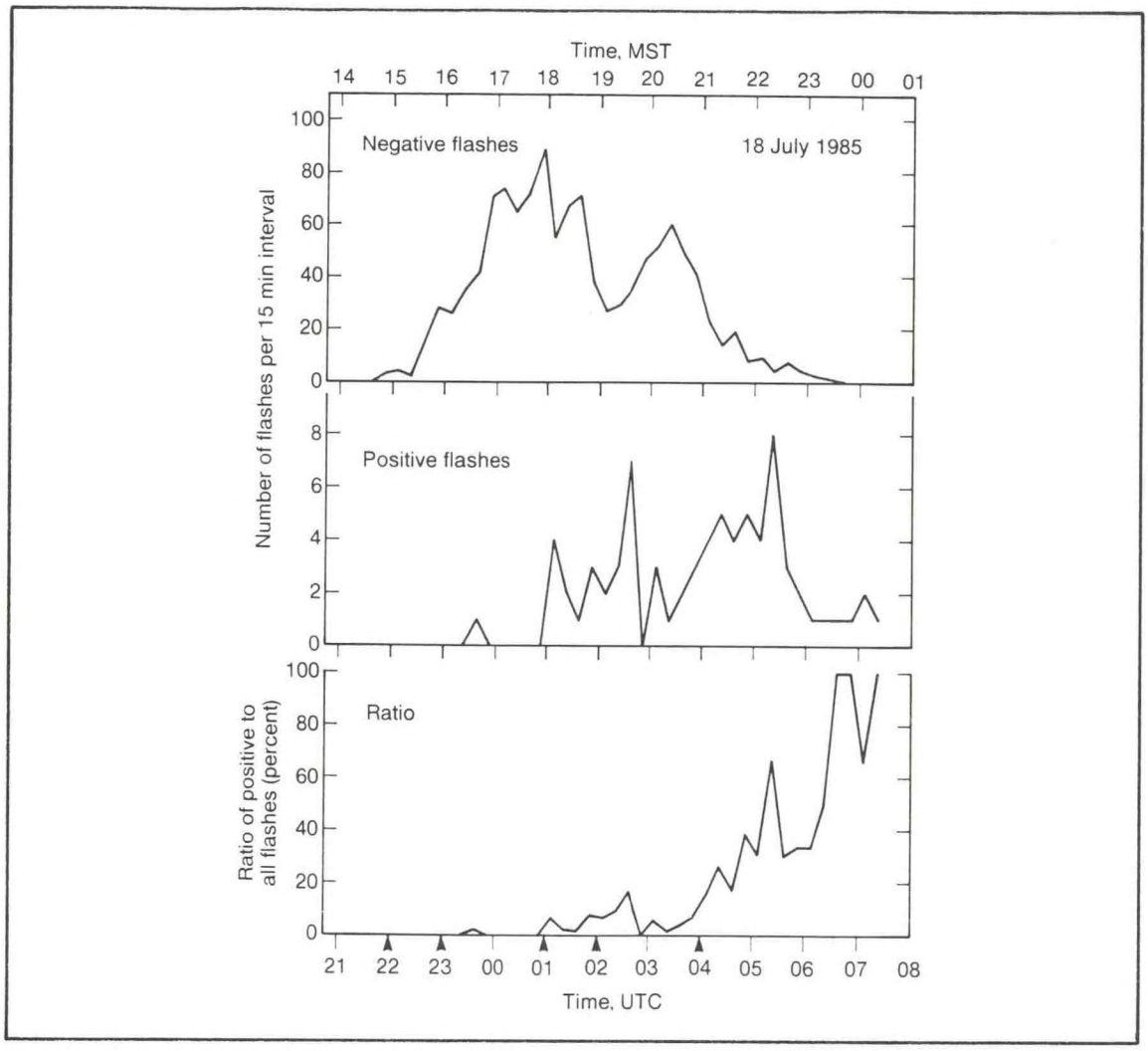

Figure 16. Time series of number of negative (upper panel) and positive (middle panel) CG flashes per 15 minutes. Lower panel shows ratios of positive to total CG flashes of both polarities in each interval. Note difference in scales between top two curves.

PRE-STORM Studies

Analysis of special PRE-STORM mesonetwork rawinsonde data that were collected at dense spatial and temporal resolution, in tandem with surrounding synoptic observations using the objective "analytic approximation" technique developed at NSSL, has allowed vertical motions occurring in and around a mature MCC to be specified in unprecedented detail. Much of our knowledge of MCC structure has come from heavily filtered composite analyses based on routine observations drawn from many storms. The mesoscale observations of the 3-4 June 1985 MCC afford a much more detailed view of one such storm, though only at maturity. Figure 17 displays representative vertical motion profiles when the mature MCC was centered in the PRE-STORM network. Each profile represents a cluster average of gridded vertical-motion values over a mesoscale subregion of the domain where similar vertical motion profiles were diagnosed. Familiar signatures associated with, for example, convective ascent, compensating subsidence, and mesoscale updraft/downdraft circulations

accompanying stratiform rainfall, as well as unique profiles along the storm's periphery were related to variations in environmental conditions, storm-environment interactions, and smaller-scale storm structure derived from Doppler radar. This diversity is consistent with a broad spectrum of weather conditions observed across the MCC and is indicative of contrasting physical mechanisms governing various parts of the storm.

Applying the dynamic retrieval method to dual-Doppler radar analyses describing an intense wake low trailing a midlatitude MCS yielded horizontal pressure gradients whose strength and orientation agree well with detailed surface observations. Previous work

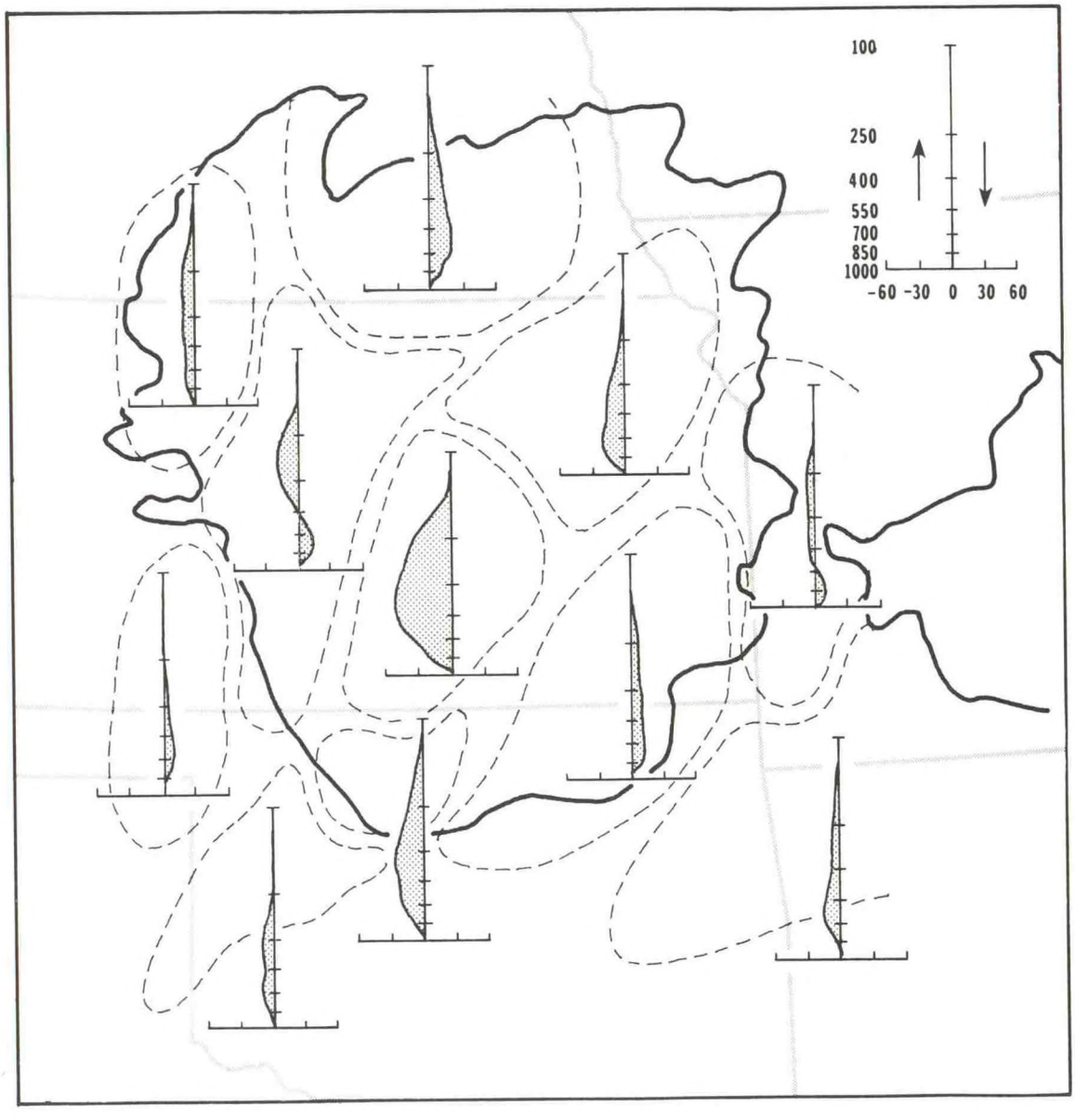

Figure 17. Profiles of mean mesoscale vertical motion in μb s^{-1}, plotted in log-pressure coordinates and averaged over representative regions (dashed lines), for a mature MCC observed over the PRE-STORM network at 0000 UTC 4 June 1985. Dark curve corresponds to satellite-observed -52°C infrared temperature contour outlining the MCC cloud-top canopy.

with CSU researchers evidenced surprisingly intense convective-scale downdrafts along the back edge of the stratiform rain area in the 3-4 June 1985 MCS. Recovered perturbation buoyancy values attest to the role of these trailing-edge downdrafts in producing extremely rapid surface pressure falls (>2 mb per 5 minutes) ahead of the wake low. Initially driven by negative buoyancy at midlevels, the downdrafts became positively buoyant as they breached the stable low-level cold pool, thus "overshooting" their equilibrium level. In tandem with warming produced by mesoscale subsidence, this more localized process contributed *hydrostatically* to surface pressure falls by eroding the near-surface layer of cold, dense convective-outflow air (Figure 18). Moreover, the intensity of these vertical motions and accompanying vertical wind shear suggests that this locale may represent a heretofore unrecognized threat to low-flying aircraft. These results are an important step toward elucidating the dynamics of the wake low and understanding more fully its relationship to the airflow and precipitation structure of the parent MCS. Future research efforts will focus on obtaining detailed measurements such as dual-Doppler scans providing more detailed descriptions of lower-tropospheric airflow, serial soundings launched from mobile platforms, and remote measurements via radiometric/acoustic systems to better address this intriguing component of MCSs.

NSSL researchers and CSU faculty studied the PRE-STORM MCS over western Kansas on 24 June 1985. Wind profiler, sounding, and Doppler radar data were used to describe the vertical structure of a midtropospheric mesovortex that developed during the decay of the MCS. Dual-Doppler analyses were completed for three times

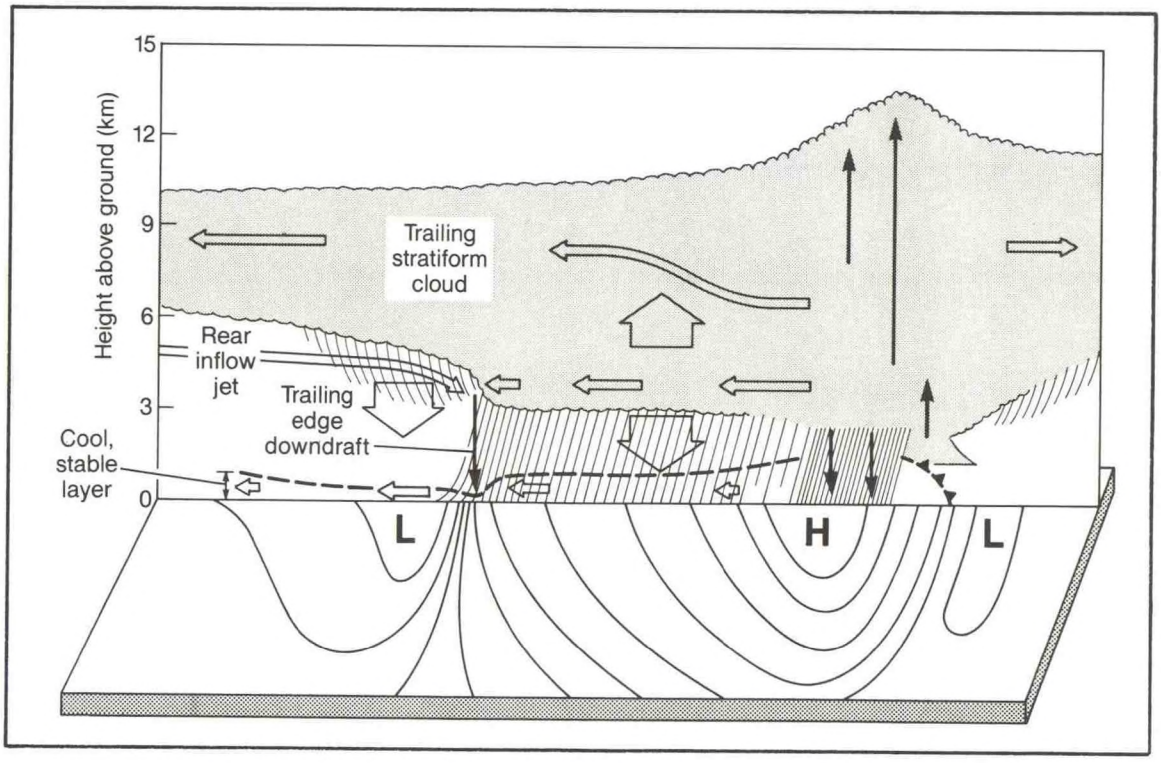

Figure 18. Conceptual model depicting the relationships of the system-relative rear inflow jet, trailing-edge downdraft, depth of the low-level stable layer, and the underlying surface pressure field in the 3-4 June 1985 MCS viewed in an east-west cross section. Storm motion is left to right. Density of hatching is proportional to precipitation intensity. The wide and narrow arrows represent mesoscale and convective-scale motions, respectively.

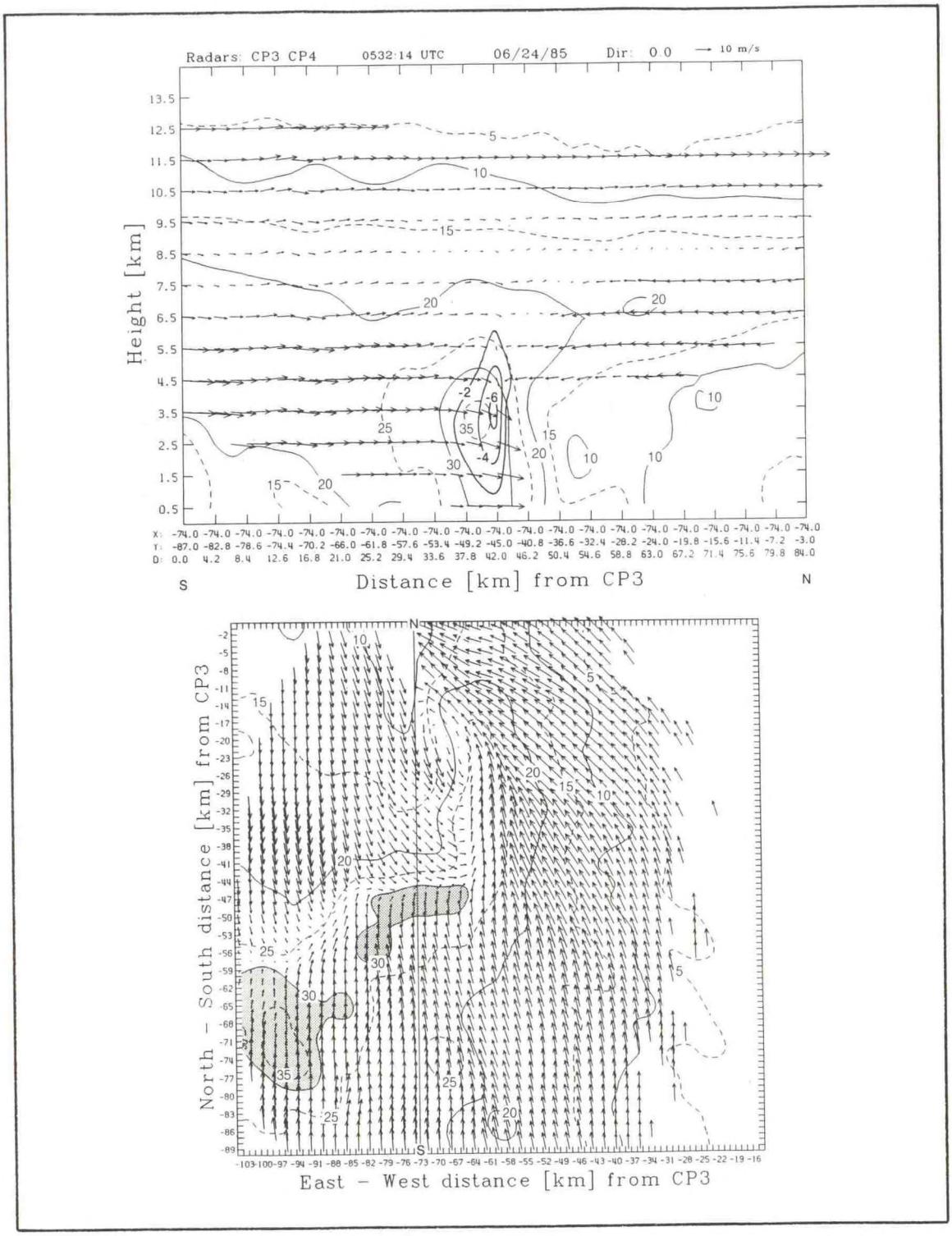

Figure 19. Analysis of mesovortex during MCS at 0533 UTC on 24 June 1985. For both panels, system-relative winds are scaled by arrow at upper right, and radar reflectivity is shown at 5 dBz intervals, starting at 5 dBz. Top panel shows north-south vertical cross section 74 km west of CP-3, and negative vertical motions less than -2 m s^{-1}. Bottom panel at 4.5 km AGL shows location of vertical cross section.

(0533, 0630, and 0723 UTC) in the region of the mesovortex. Figure 19 shows a closed cyclonic circulation centered just west of the north-south precipitation appendage. There is a strong suggestion that the mesovortex itself was creating the hook-like reflectivity pattern by carrying hydrometeors northward on its east side and eroding them on the west, perhaps through evaporation. A north-south cross section of reflectivity and system-relative winds just west of the mesovortex center shows a pronounced zone of mid-tropospheric convergence of front-to-rear flow from the south, with rear-to-front flow, also called the rear inflow jet, from the north. This converging flow descended with speeds up to 6 m s^{-1} in a narrow zone about 10 km wide collocated with a band of intense surface pressure gradients. This pattern shows a remarkable resemblance to that observed at the rear of a trailing stratiform region that occurred over Kansas on 3-4 June 1985. These cases illustrate the dynamical consequences of stratiform precipitation regions.

Spatial patterns of CG flashes relative to radar echo type and severe weather were determined for the second of the four 3-4 June MCSs during PRE-STORM. The lightning activity consisted mostly of negative CG flashes coincident with convective radar echoes in short, intense lines as the lines grew. As the storm matured, negative flashes were concentrated in the convective area, then positive flashes began to increase in number, mainly in the stratiform area. Figure 20 shows the distribution of CG flashes throughout the life cycle of MCS II in the analysis area. The dominant feature is the large grouping of negative flashes in convective echoes over northern Oklahoma and Kansas. Several locations had up to 30 or more flashes in an area of 156 km^2 during this storm. Negative flashes in stratiform echoes were relatively scarce. Positive flashes tended to concentrate in the same convective regions as negative flashes, although they were more widely dispersed in stratiform areas. The 10 cases of severe weather during

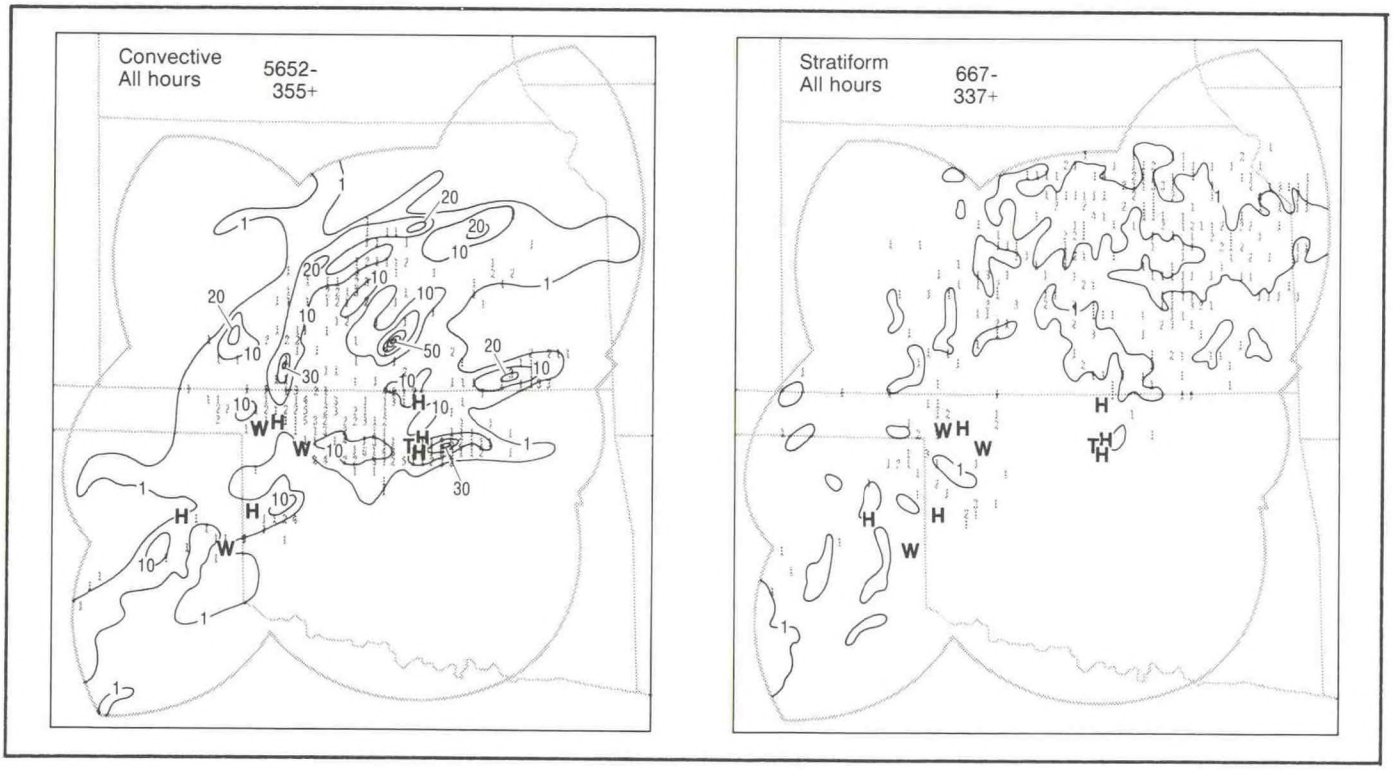

Figure 20. Horizontal maps of CG lightning flashes during the entire life cycle of MCS II. Contours show negative flash density per grid square of 12.5 by 12.5 km (156 km^2). Positive flashes are shown as number per grid square. Severe weather events indicated by H=hail, W=wind, and T=tornado.

this MCS were concentrated on the southern and western sides of the MCS, where there were large concentrations of negative flashes within the convective radar echoes.

Retrieval Methods

Air motion fields, pressure and temperature fields, and pressure and temperature tendency fields were deduced from Doppler radar data for the MCS of 3 June 1989, which was observed as part of COPS–89. The system was dissipating at the time. A sharp, sloping shear zone in the stratiform region was becoming more horizontal. The mesoscale updraft in the upper half of the stratiform region was weakening. Pressure was changing at middle levels to weaken the existing pressure gradient that was accelerating air into the system from the rear. These pressure changes were associated entirely with temperature changes at lower levels, which were associated with air descending and warming in regions of little precipitation, but cooling when it flowed through the main rain shaft in the stratiform region. This study shows that intensity of precipitation in the stratiform region affects whether heating or cooling occurs in the mesoscale subsidence, and that the pattern of heating and cooling in the layer of subsidence affects the pressure forces and evolution of the flow in the middle levels.

Q-Vector Analysis

A generalized Q vector was developed, starting from the primitive equations and using minimal assumptions. The divergence of this Q vector is a simple generalization of several well-known versions of the forcing function for vertical motion that have been developed by Sutcliffe, Trenberth, Hoskins and Keyser. The basic assumption of this approach leads to a set of filtered, "alternative balance" equations, which, in principle, may be applied to shock-free initialization of limited-area, primitive-equation forecast models by solving for the three wind components given the observed temperature field.

Nighttime Rainfall in the Central United States

NSSL continues to study the environments that lead to the pronounced climatological maximum of nighttime rainfall and thunderstorms over the central United States. We still do not understand well the interplay of large-scale and mesoscale processes that leads to nighttime rains over the Plains, and the accurate prediction of such rains remains elusive.

The July hourly precipitation records for Omaha, Nebraska, for 1958-1987 were used to identify nocturnal rain events that produced at least 0.25 inches of rainfall. We restricted our attention to rain events that commenced between 0000 and 1200 UTC and ended by 1800 UTC. For the 30-year period examined, 67 such nighttime precipitation events were identified; the frequency of occurrence of such events in July is thus slightly more than 7%. A mean 850-mb chart (Figure 21) illustrates conditions that preceded heavy nocturnal rain events at Omaha during July. This analysis illustrates the strong southwest-northeast temperature gradient that extends from Iowa to Colorado and New Mexico, indicating that substantial warm advection in the lower troposphere is a key feature of the supportive environment. These studies will continue for several other stations that have pronounced nighttime rainfall signatures in their climatological record, and will also be expanded to consider null-case composites.

GUFMEX Studies

NSSL led the GUFMEX field program in 1988 that investigated moisture return from the Gulf of Mexico in the cool season (February-March). Continuing minor field exercises in the ocean environment are planned to evaluate instrumentation related to flux measurements and sense the water vapor content of near-surface layers. Mobil Oil has allowed an oil platform near the edge of the continental shelf to be used for such evaluations.

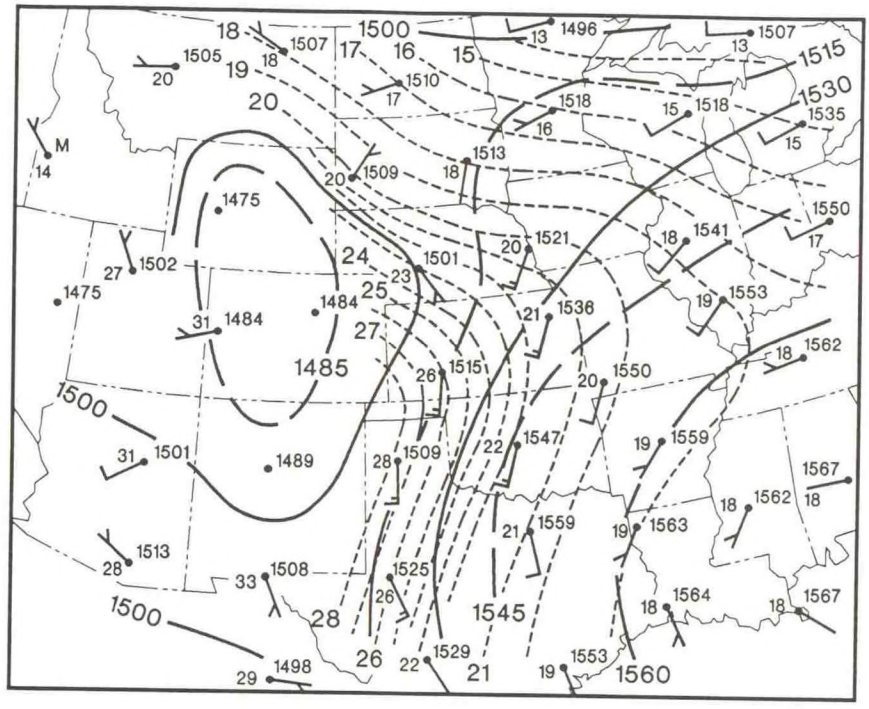

Figure 21. Mean 850-mb chart for 0000 UTC preceding 67 nocturnal rain events at Omaha, Nebraska. Height contours (m) are solid lines, and dashed lines are isotherms (°C).

The first round of research using these data was reported at the Air-Sea Interaction and Air Mass Modification Symposium held at Galveston, Texas, in January 1991. The symposium was sponsored by a new NWS cooperative institute at Texas A&M University, the Cooperative Institute for Applied Meteorological Studies. A wide range of research is under way.

Modeling

- Mixed layer - CIMMS
- Regional with detailed PBL - Navy
- Synoptic with telescoping - Canada
- Cumulus with PBL - University of California

Case Studies

- Mixed return flow - University of Wisconsin
- GUFMEX trajectories - NSSL
- Climatology - NSSL
- Operational assessment in the severe storm outlooks - NSSFC
- NMC model performance - Texas A&M

Satellite Studies

- Microwave and infrared imagery - University of Wisconsin
- Data assimilation - University of Wisconsin

One project at the University of Wisconsin was designed to explore the accuracy and usefulness of microwave satellite moisture and wind data in synoptic analysis over a normally data-sparse region, which for this study was enhanced with additional surface and upper-air observations during GUFMEX. The microwave data are from the Special Sensor Microwave/Imager (SSM/I) aboard the Defense Meteorological Satellite Program (DMSP) satellite. Precipitable water and wind-speed magnitudes were estimated during cold-air outbreak/return-flow episodes in the Gulf of Mexico, with differences in precipitable water from rawinsondes similar to those found in previous studies that had larger and more diverse observation sets. For the first time, intercomparisons were made between precipitable water estimates from GOES-Vertical Atmospheric Sounder (VAS) and SSM/I instruments. Both instruments revealed the major synoptic features during the period of observation. The information available from satellites must be readily assimilated by both forecasters and forecast

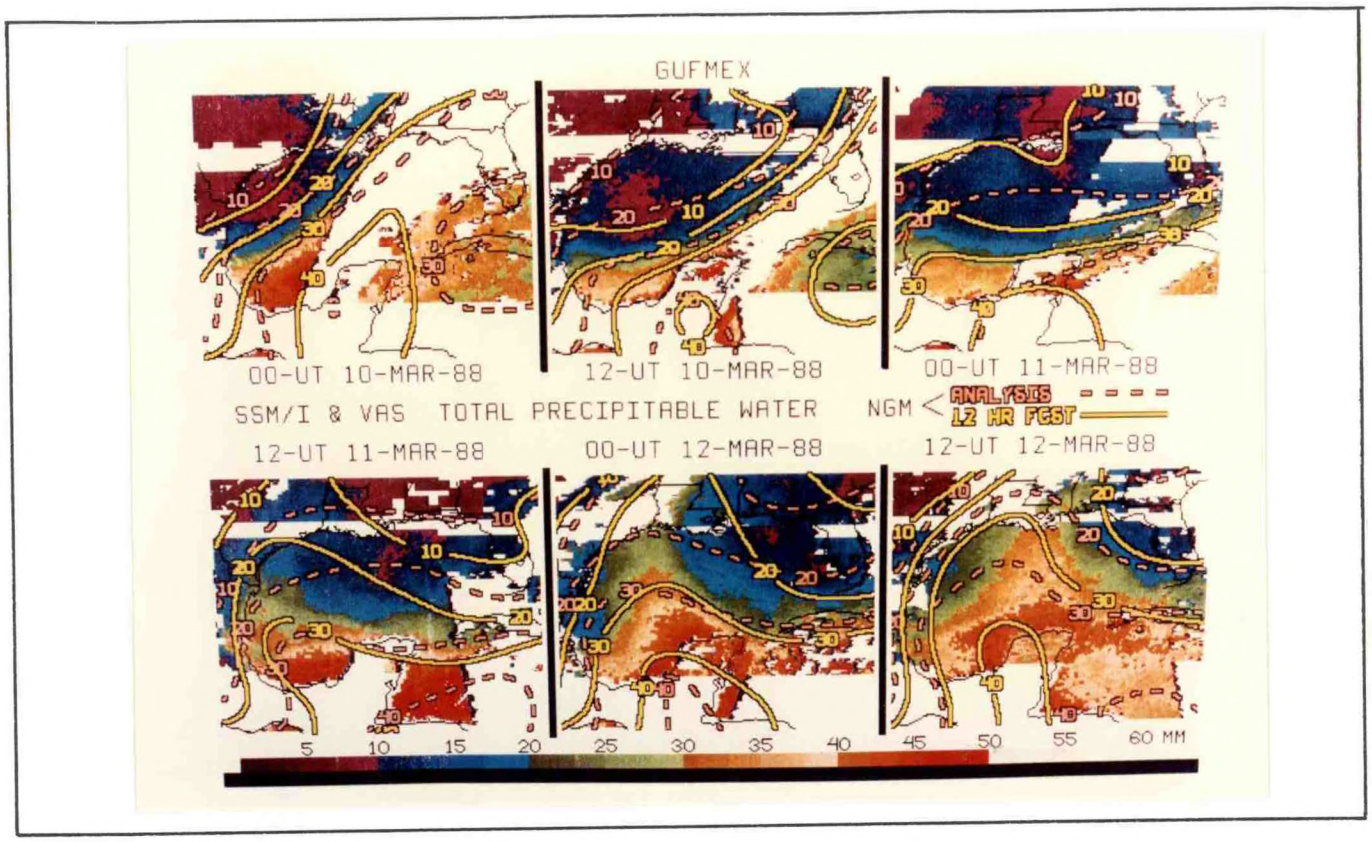

Figure 22. Composite analyses of precipitable water from SSM/I and VAS satellite data. Contours give precipitable water values for both 0-hour initializations and 12-hour forecasts from the NMC operational NGM. Contour values correspond to color changes indicated in the bottom scale. Based on advantages of the microwave data, VAS data are shown only where SSM/I data are unavailable, such as over land.

models if it is to be useful in weather prediction. For example, Figure 22 is an attempt to combine VAS and SSM/I satellite data with forecast model output.

Results of this study will guide the use of future microwave satellite instruments such as AMSU-B in the 1990s. To address the global water budget for the continental-scale experiment of the Global Energy and Water Cycle Experiment (GEWEX), future work will use satellite moisture data to estimate regional atmospheric moisture budgets. Figure 23 shows the atmospheric water-vapor storage term during a 12-day period over the Gulf of Mexico determined from SSM/I data and Nested Grid Model (NGM) forecasts.

ERBE

For the Earth Radiation Budget Experiment (ERBE), cloud feedback and earth-surface characteristics on the earth/atmosphere radiation budget were assessed from regional satellite observations. Feedback of clouds is an important factor in anticipating the effect of increasing carbon monoxide on climate. In collaboration with the NESDIS Cooperative Institute for

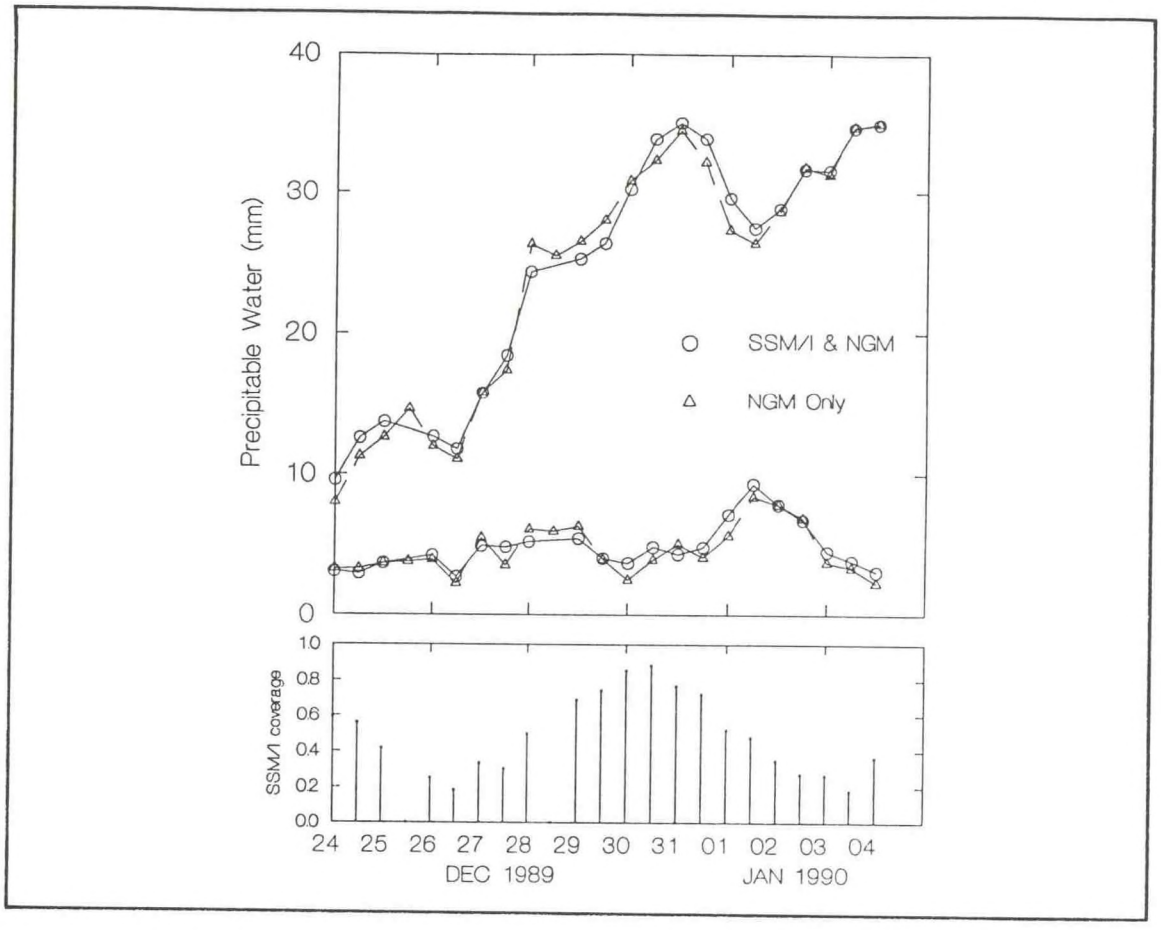

Figure 23. Precipitable water averaged over the entire Gulf of Mexico. Mean (upper two curves) and standard deviation (lower two curves) from NGM 12-hour forecasts only, and with the addition of SSM/I data. Vertical bars (bottom) give fraction of the gulf covered with SSM/I data. Forecast and satellite information appear to depict the mean atmospheric water storage quite well. Estimates of evaporation and flux divergence of water vapor are required to evaluate the entire regional water-vapor budget.

Meteorological Satellite Studies (CIMSS) in Madison, Wisconsin, efforts have continued to examine the impact of deep convective clouds on the radiative energy absorbed by the atmosphere over North America during the warm season. The mean hourly net radiation at the top of the atmosphere and the effects of deep convective clouds are shown in Figure 24. The greenhouse (warming) effect of cold-top clouds at night approximately offsets their cooling effect during daylight hours when the observed nocturnal maximum of such cloud cover is considered. However, the amount and sign of the effect of deep convective clouds on the radiation balance was found to be quite sensitive to the diurnal distribution of these clouds. Hence, the diurnal cycle of clouds must be accurately measured or simulated to assess correctly the feedback of clouds. The monthly effect of deep convective clouds on the regional radiation budget does not seem large, especially compared to the potential effect of low clouds and the latent heat release accompanying storms. However, the long-term effects must still be considered, along with many other components, such as water vapor, land surfaces, greenhouse gases, and solar fluctuations, for a comprehensive understanding of the Earth's climate system.

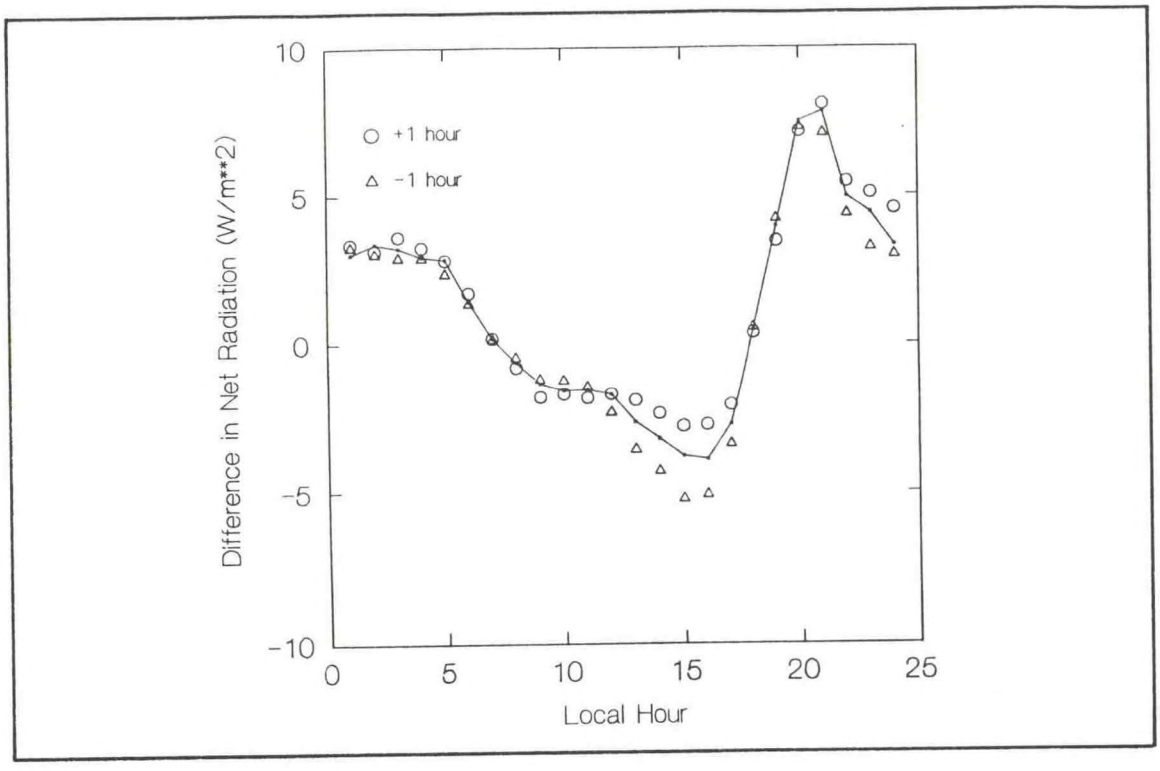

Figure 24. Difference over time in monthly mean net radiation due to the presence of deep convective clouds. Circles and triangles indicate values if the coverage of convective clouds is phase shifted forward or backward by 1 hour.

Large-Scale Climatological Means

The Forecast Systems Laboratory (FSL) and NSSL jointly have compiled a data base of about 40 years of upper-atmospheric soundings for North America. This data base is expected to be very useful in studies of climate change. For example, 30-year averages were compiled at NSSL for each Julian day of the year, for the two sounding times of 0000 and 1200 UTC, from 1958 to 1978. These averages were produced for the five standard sounding data fields at mandatory level plus others, for a total of 21 levels. In addition, there is a comparable record of precipitation in the NSSL-FSL archive and in a separate archive available from the Climate Monitoring and Diagnostics Laboratory (CMDL). As a simple exercise, data from average soundings for various months were used to compute quasi-geostrophic forcing patterns for the western portion of the United States. For example, at 700 mb (Figure 25), there is an elongated area of average ascent extending from northeastern Colorado along the Kansas-Nebraska border into Iowa that corresponds to the average MCC trajectory for June. The corresponding average precipitation reflects the available moisture flux in its east-west gradient, but it also reflects upper-level forcing patterns.

Figure 25. Quasi-geostrophic analysis at 700 mb from 30-year average upper-air data against a background of terrain elevation (solid colors) having thresholds at 3-km intervals. Height field analysis is depicted through white contours at intervals of 20 m. Yellow contours depict the divergence of Q-vectors that is the forcing term in the omega equation; dotted contours represent negative values (upward forcing), solid contours represent positive values (downward forcing), and dashed contours represent zero values. Red contours depict the temperature field at 1°C intervals.

Hail Growth Studies

Microphysical processes were related to kinematic fields in a severe hailstorm that occurred in Denver on 13 June 1984 and caused numerous injuries and more than $350 million in damage. Polarization variables allowed identification of regions with rain, hail, and mixed phase of both liquid and frozen particles, and subsequent estimation of the fall velocities of these hydrometeors. Dual-Doppler analysis and terminal fall speeds were used to reconstruct particle trajectories in the storm. Of particular significance was the discovery of a column of high differential reflectivity, ZDR, that extended well above the freezing level. This column had an important role in influencing hail embryos and hail growth.

The column consisted of drops having median diameters of about 2 mm, and extended to about 2 km above freezing level. It was offset northwest from the updraft center, which coincided with a weak reflectivity notch (vault). Thus, hydrometeors in the updraft center were swept into the upper part of the storm too quickly for in situ growth of hailstones, but because the column coincided with weaker updrafts, this weaker draft region supported the sizable rain drops.

Three major trajectories accounted for most hydrometeor paths that formed the column. All the trajectories originated in the southwestern part of the storm and fell cyclonically through the reflectivity overhang. Some carried particles to the downwind anvil and out of the storm, some contained hydrometeors that fell as rain, and some may have recirculated hydrometeors as frozen drop hailstone embryos. The drops responsible for the ZDR column appear to have originated as ice crystals that fell from the backshear anvil and then melted. Trajectory analysis suggests that the existence of the lowest part of the column below the freezing level was due to the proximity of the melting level to the low-level cyclonic flow; i.e., frozen hydrometeors descended, melted, and were caught by the cyclonic airflow into the updraft. Above the freezing level, the column consisted of melted hydrometeors advected upward by the lower velocities of the western updraft flank.

Two distinct hail fallout regions, northern and southern, were found. In the northern area, growth was "from scratch," where most mass was acquired as embryos crossed the column, or the embryos grew as they were carried over the vault. Hailstone paths in the southern region tended to descend cyclonically from the same southwestern part of the storm as did the hydrometeors that formed the ZDR column (Figure 26). The hailstones either fell through the column (trajectory A), where they acquired most of their mass, or passed through the vault (trajectory B). Calculations of surface hail sizes show this to be a fallout area of the largest (6-cm) hail.

There are distinct differences between the ZDR column reported here and previous studies. The columns observed in the Southern Plains of the United States and in England were caused by a warm-rain coalescence process. Consequently they contained high ZDR (4-6 dB) values and no surface hail. Lower elevation in these regions, higher AGL freezing levels, and larger liquid water content in the updraft are the main causes for the difference.

Splitting Thunderstorms

Analyses are under way of three splitting thunderstorms that occurred in southern North Dakota on 27 June 1989, during the North Dakota Thunderstorm Project. Two storms were sampled intermittently with a ground-based and airborne dual-Doppler radar configuration. The third storm was sampled by two ground-based Doppler radars from initiation through the beginning of the splitting process. These splitting storms are unusual because the left-moving storms were larger and longer lasting than their right-moving counterparts. Preliminary analyses of the first two storms indicate that the

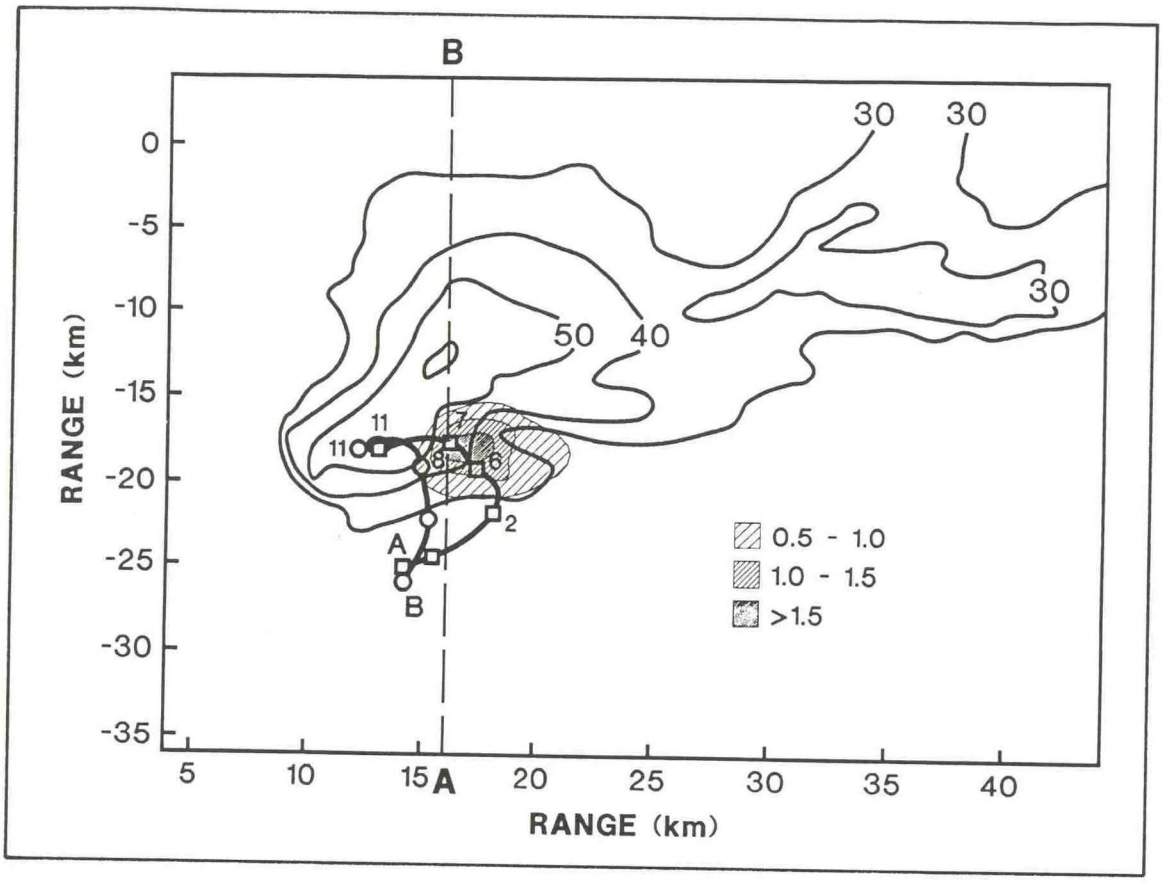

Figure 26. Projection at 3.5 km AGL of trajectory A, which ends in the southern hail region. Path A directly crosses the column. Reflectivity is contoured at 10 dBZ increments. Differential reflectivity of the column is hatched at 0.5 dB increments. Range is relative to the NCAR CP-2 radar. Values of dual frequency ratios (dB) at 4-minute intervals are indicated along the trajectory. This parameter is a ratio of a reflectivity factor for a 10-cm wavelength and a reflectivity factor for a 3-cm wavelength; values above 6 dB are reliable indicators of hail. The ratio increases rapidly as the hail's paths descend through their growth regions.

splitting process was not continuous, as had been hypothesized by previous investigators, but was due to the formation of a series of new updrafts on the storms' lateral flanks. Dual-Doppler analyses of the third storm should reveal how within-storm processes become organized to initiate the splitting mechanism.

NOAA Satellite Channel 3

The so-called "channel 3" information provided by the NOAA polar-orbiter spacecraft is situated in the electromagnetic spectrum where it represents a mixture of thermal and reflected radiation. This channel has not seen a great deal of use in studying convective storms, although it has other applications. Recently, however, in collaboration with the Czech Hydrometeorological Institute (Prague, Czechoslovakia), exploration of the data from channel 3 has revealed that some thunderstorm tops exhibit enhanced reflectivity in this channel that can be distinguished clearly from emitted radiation using techniques developed in Czechoslovakia. The enhanced channel-3 reflectivity takes on one of two structures: a clearly defined cellular area or a plume-like structure. Occasionally, both can be seen at the same time.

There are some early indications that the signatures seen in such data as Figure 27 might be associated with hailstorms, although this association has not yet been validated. Why cloud top reflectivity is enhanced is not known, but it is probably related to the type of cloud particles in the storm top. Further exploration of these data should shed light on how effectively this signature can discriminate among severe and nonsevere storms, as well as how the signatures are created.

Relative Dry Microburst Threat at Western Airports

The relative threat of dry microbursts was computed from average soundings in the FSL/NSSL historical archive of North American soundings for a 30-year period ending in 1988. Various parameters extracted from these average soundings, such as the 700-500 mb lapse rates and 500-mb moisture mixing ratios, were input into a predictive linear model (by Caracena and Flueck) using preconvective soundings taken during the JAWS project in the summer of 1982. The predictive model was calibrated during the convectively active season along the Front Range of Colorado during a very convectively active year. Therefore, the curves probably

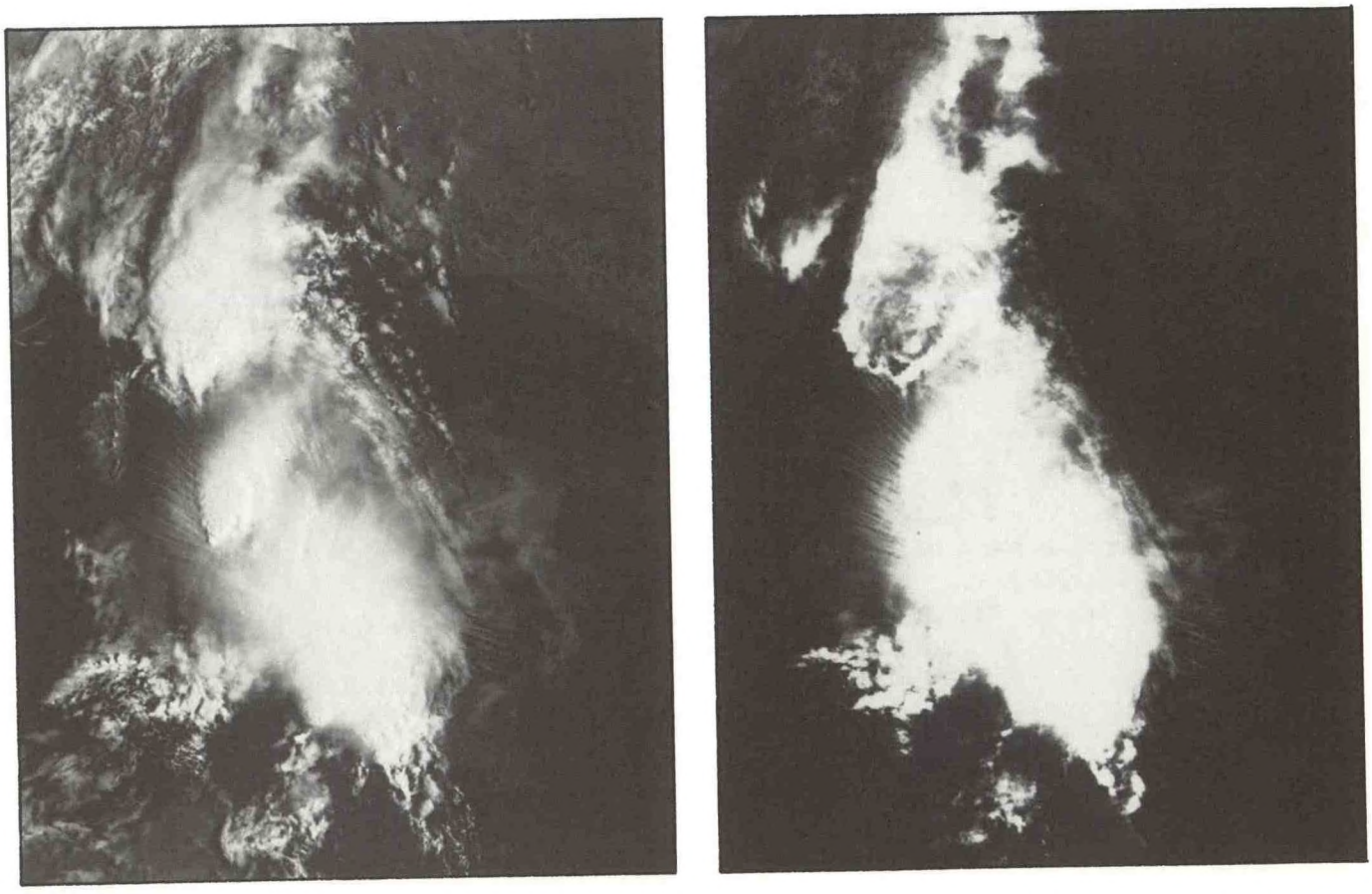

Figure 27. Comparison of NOAA-10 satellite AVHRR visible channel 2 (left) and AVHRR channel-3 enhanced reflectivity (right) at 0630 UTC 1 September 1990 over Eastern Europe.

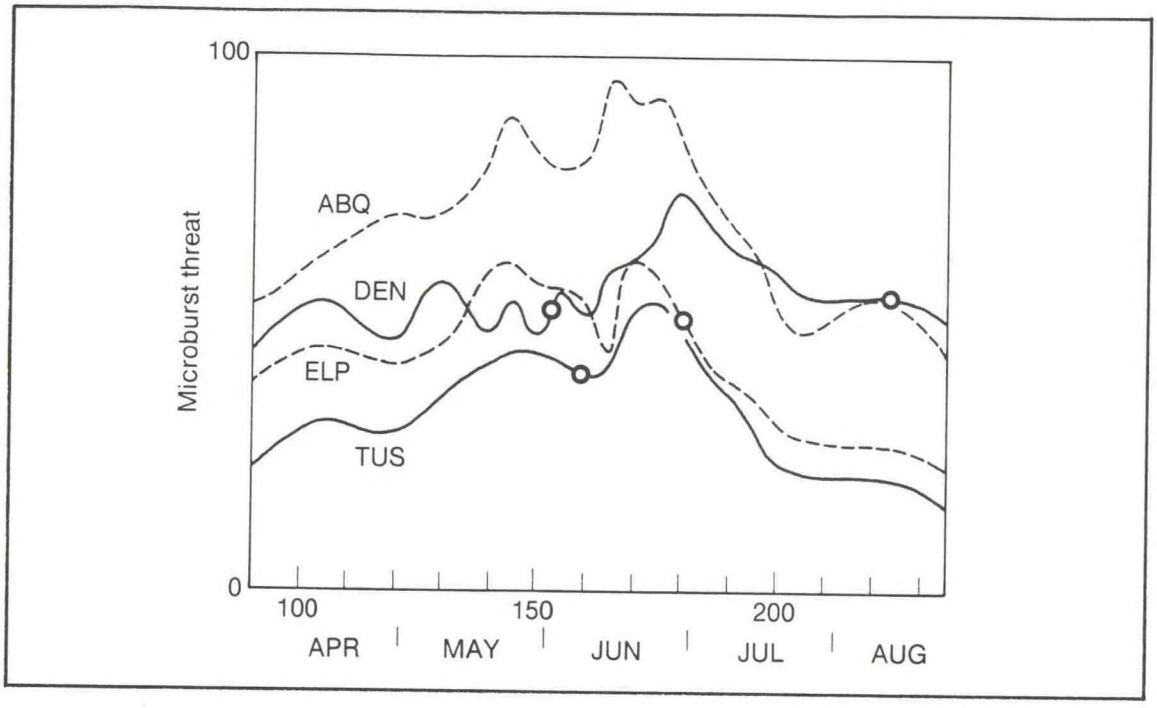

Figure 28. The relative threat of dry microbursts for various western U.S. sounding stations computed from 30-year average soundings at each site using a predictive linear model. Times of year (Julian days plotted across bottom) and places where dry microburst accidents have happened are shown by large dots.

represent the conditional probability that microbursts will happen, given that convection is going to occur. If so, the real threat of microbursts before the onset of the convective season in the western states is probably much smaller than indicated in Figure 28 before June, but correctly depicted during the summer. Therefore, the relative probability of dry microbursts should peak much more sharply than shown during the last half of June, because without convection, the relative probability of dry microburst occurrence is dragged down to almost zero for the first half of the period of Figure 28.

Improvements to NOAA P-3 Doppler Radar

A new technique has been developed to derive dual-Doppler wind fields using the NOAA P-3's airborne Doppler radar. This fore/aft scanning technique, or FAST, utilizes the capability of the current tail-mounted antenna to scan forward or aft of the aircraft to view a region of space from two vantage points along a single, straight-line flight track (Figure 29). For each beam intersection point, a horizontal wind estimate can be calculated from the two observations of radial velocity. The horizontal density of points is reduced about 50% (to about 2 km) over the previous technique of flying two quasi-orthogonal flight legs with the antenna scanning normal to the track or toward only one side of the aircraft. The major advantage of FAST is that data are collected in roughly one-half the time of the previous technique, mitigating some of the deleterious effects of the weather system evolving during data collection. There also can be situations, such as when flying near long squall lines or because of air traffic control restrictions, where it is impossible to fly an L-shaped flight pattern. The accuracy of the FAST wind field is not seriously compromised because the beam intersection angles are reduced from 90° to about 50°. Normally, radial velocity data are also contaminated by the aircraft's ground speed, resulting in an additional step in the editing of the data. FAST was used during the Southwest Area Monsoon Project (SWAMP) project in 1990 to examine the kinematic structure of MCSs with great success, and will probably be the standard method of collecting airborne Doppler radar data in the future.

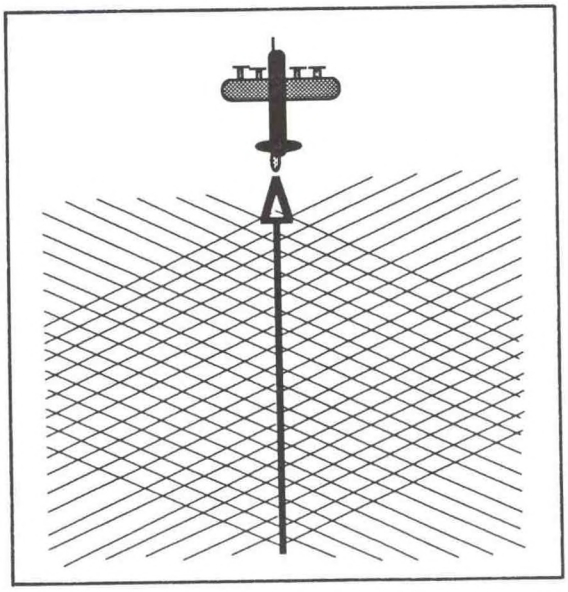

Figure 29. The horizontal distribution of beams using the fore/aft scanning technique (FAST).

As a result of negotiations between NSSL staff and representatives of the French research group Centre de Recherches en Physique de L'Environnement Terrestre et Planetaire (CRPE), NOAA has joined with the French to build a phased array, dual-beam antenna for the P-3. Under this agreement, the French will build the antenna and NOAA will install it on the P-3 for the TOGA-COARE project. Advantages of this antenna over the current one are improved sidelobe performance and quick switching of beams from fore to aft, compared to the current mechanically steered antenna, resulting in better data coverage. The new antenna will also allow for future development of a simultaneous dual-beam coverage through the use of a second radar, resulting in improved spatial resolution.

SWAMP

The Southwest Area Monsoon Project (SWAMP) was conducted during July and August 1990 over Arizona and northern Mexico (Figure 30). The project was a cooperative effort among NSSL, NWS, Mexican government research agencies, and the Salt River Project (SRP) in exploratory field data gathering. Major accomplishments of the project operations included the following:

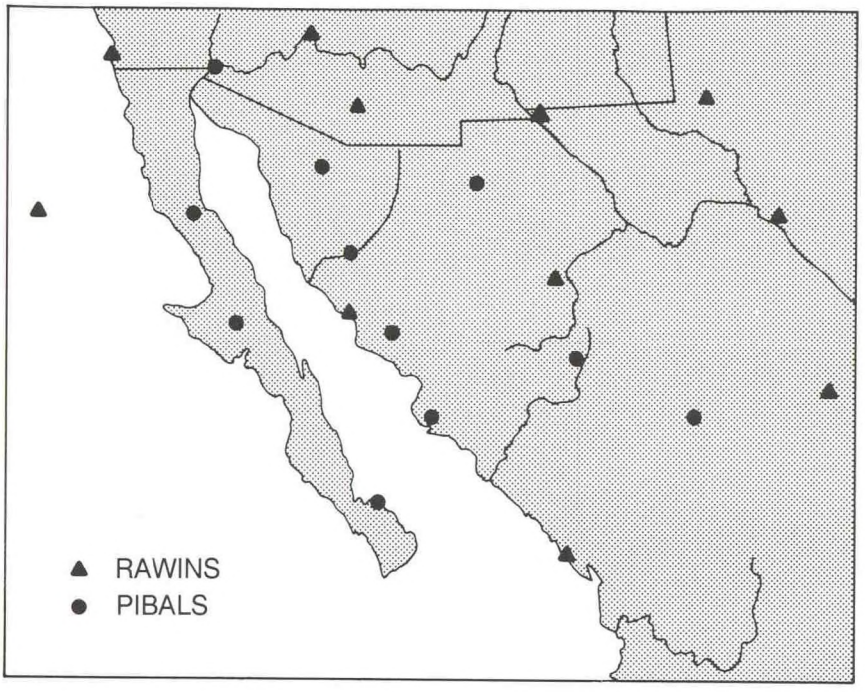

Figure 30. Locations of upper-air stations during SWAMP.

- The NOAA P-3 aircraft flew 13 research missions during the project and gathered approximately 75 hours of data on the structure of convective weather systems over Arizona and Mexico, the monsoon boundary, and the structure of the monsoon.
- Upper-air CLASS soundings were taken at the Phoenix airport every day of the project in a variety of thunderstorm environments.
- The NSSL mobile laboratory was used to document the nighttime evolution of the three-dimensional structure of temperature and moisture over the Salt River Valley in central Arizona, thereby providing data on the Phoenix heat island and the local thunderstorm environment.
- Upper-air soundings were gathered on 5 days over northwestern Mexico and the southwestern United States to enhance the resolution of observations of the large-scale monsoon structure.
- Pilot balloon wind soundings were taken daily at 10 locations in Mexico to document circulations over the Gulf of California that lead to influxes of moisture into Arizona and California.
- The new technique to allow construction of dual-Doppler wind fields from straight-line flight tracks, FAST, was used for the first time.
- In support of studies of convective systems and moisture flux calculations, 17 Omegasondes were dropped over northwestern Mexico and the Gulf of California.
- Data were gathered within five MCSs over Mexico to allow comparison with their midlatitude counterparts and assessment of their roles within the larger-scale monsoon flow.

Specific activities related to the research goals of SWAMP included the following:

- Support for initial studies of regional climate processes during the summer over southwestern North America.
- Help in defining the atmospheric structures of the "monsoon boundary," the interface between the moisture-laden air of subtropical-to-tropical origins and the dry, subsiding air over the eastern Pacific.

- Support for initial studies of cloud and precipitation systems, particularly thunderstorm complexes that are embedded within the monsoon flow.
- Provision of unique in-situ data over central Arizona to help define the local thunderstorm environment during the monsoon period, and eventually improve storm warnings and forecasts in Arizona and other parts of the western United States.

During SWAMP, the NOAA P-3 tail radar antenna used FAST by slewing 23° forward, then aft, of the flight track during alternate vertical scans. One of the first research applications of this technique involves a preliminary study of a small convective system that developed south of Phoenix, Arizona, on the evening of 1 August 1990. This system caused pea-sized hail, strong winds, heavy rains, and the coolest temperature at Phoenix during SWAMP. Unique problems were encountered because the radar data were collected over the complex terrain of Arizona. Pressure altitude rather than radar altitude had to be used to determine the height of the data, and the ground had to be manually removed. An example of a low-level analysis of winds and reflectivity along an east-west-oriented line of storms is shown in Figure 31. The lack of a strong inflow to the storms, together with mainly downward vertical motion, suggests these storms were sampled during their dissipating stage. Future analyses of this system will focus on a north-south-oriented line of storms and a residual area of stratiform precipitation.

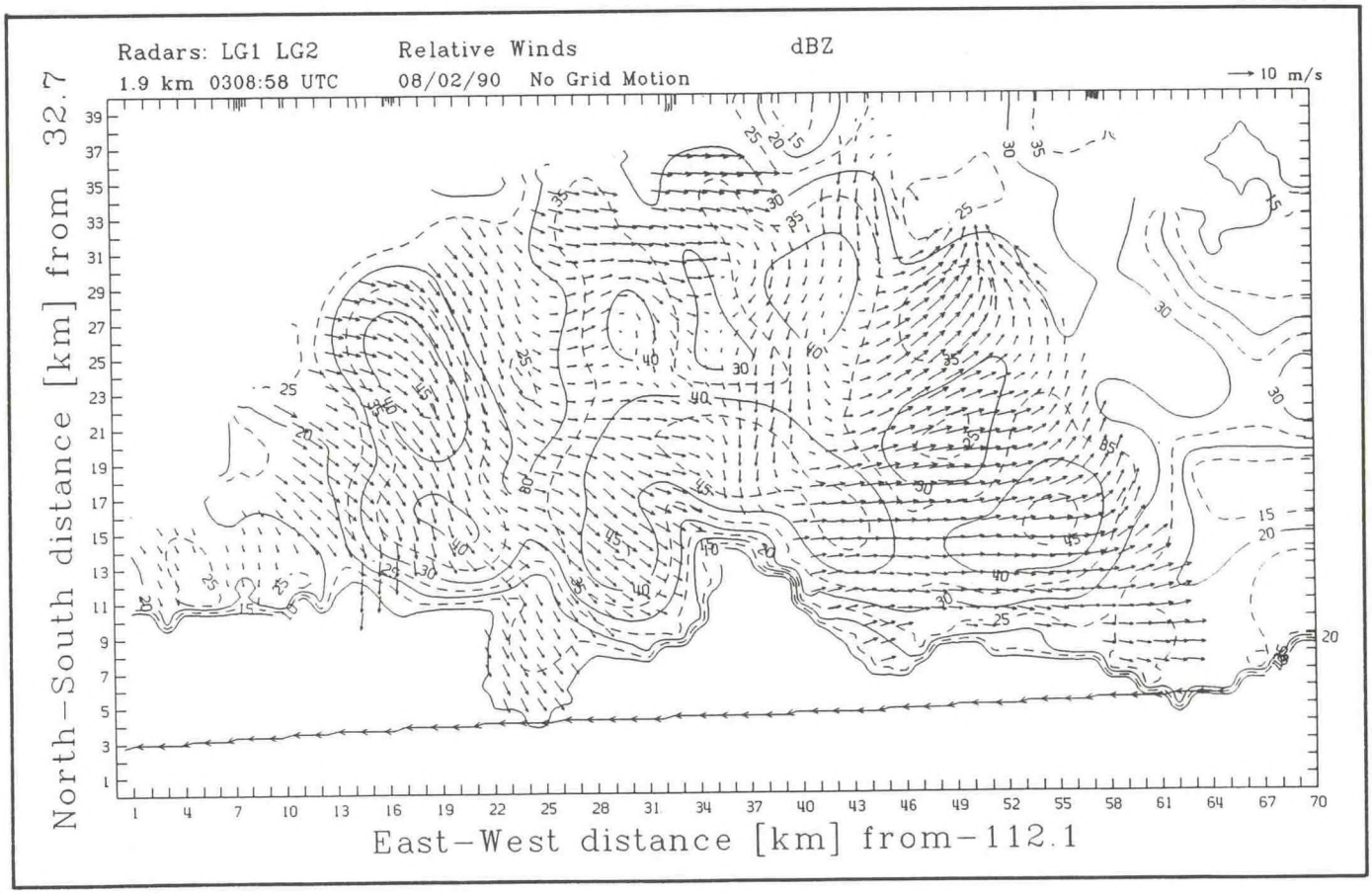

Figure 31. Horizontal plot at 1.9 km MSL of winds and reflectivity derived from FAST at 0309 UTC 2 August 1990. Wind vectors are relative to the earth (no system motion).

A pilot balloon (pibal) network was established to provide a temporally near-continuous depiction of the wind field at meso-alpha-scale resolution in the vicinity of the mesoscale weather systems being investigated by the NOAA P-3. Ten pibal stations were operated between 5 July and 15 August 1990 in seven Mexican states (Figure 30). More than 1000 soundings were obtained using NSSL-provided 100-gram balloons and theodolites on loan from the NWS. The Servicio Meteorologico Nacional (SMN) de Mexico provided most of the personnel needed to make the pibal observations taken three to four times daily, with help from several Mexican research institutions. These personnel were trained during a short course held in Hermosillo, Sonora, before the experiment. The SMN also provided the hydrogen gas needed for balloon inflation. A station was also established on short notice in Yuma, Arizona, where twice-daily soundings proved crucial in monitoring the surges in low-level flow into the southwestern U.S. deserts during SWAMP. The raw pibal data, recorded on specially provided forms, are being transferred to disk and thoroughly checked for recording and key-punching errors. These data should provide the best description to date of the wind field associated with the southwest monsoon over the North American deserts.

The SRP and NSSL joined in an intensive data-gathering effort during SWAMP to investigate the three-dimensional structure of the Phoenix heat island. Four missions were conducted with NSSL's M-CLASS and with a fixed version of the system. Soundings were released every 30 minutes during several traverses across the Phoenix metropolitan area by the M-CLASS. The fixed site at the NWS office released extra soundings in conjunction with the mobile platform. Each mission was conducted from the late evening hours through the next morning. Over the next year, the SRP and NWS will conduct a joint study of the data collected.

MCSs over the high terrain of Mexico are an apparent mechanism for vertical transport of moisture that is eventually advected northward by the monsoonal circulation. The existence of these MCSs has recently been noted from satellite imagery, but very little is known of their internal kinematic and precipitation structures. Airborne Doppler data collected during SWAMP, however, allow us to document the internal characteristics and evolution of these transient systems. Our first study focused on the Mexican MCS of 20 July 1990. The MCS consisted of a 150-km-long, bow-shaped convective line with an especially intense convective cell on its northern end (Figure 32) and a region of stratiform precipitation to the south-southwest of the line. Embedded within climatologically favored easterly flow, the squall line had a zone of strong midlevel convergence that apparently resulted in a series of downdrafts on the line's western side. Outflows from the downdrafts of the individual convective cells, which formed over the high terrain to the west of the Sierra Madre Occidental range, may have played a role in the initiation and organization of the larger-scale system. Preliminary analyses also indicate that summer convection over the Mexican high terrain may be as intense as that observed over the U.S. Great Plains. Cloud-top heights to 18 km were observed, and vertical velocity calculations indicated updrafts of greater than 20 m s^{-1}. Analyses of this and other SWAMP MCSs will continue to be compared to mesoscale convective patterns that have been documented for both the tropics and the midlatitudes of the Great Plains. The role these MCSs play in the monsoonal circulation will also be investigated.

Cloud-to-ground lightning positions for the SWAMP period were obtained from a network operated by the U.S. Bureau of Land Management (BLM) and from the Lightning Location and Protection, Inc. (LLP), low-gain test network in the Tucson, Arizona, metropolitan area. The BLM network contains 36 magnetic direction finders covering the western United States. A preliminary study summarized the high-lightning period of 19-24 July, when 80,602 flashes were detected across Arizona (Figure 33). In contrast, only 1795 flashes were detected during the low-lightning period of 25-30 July across Arizona. The principal

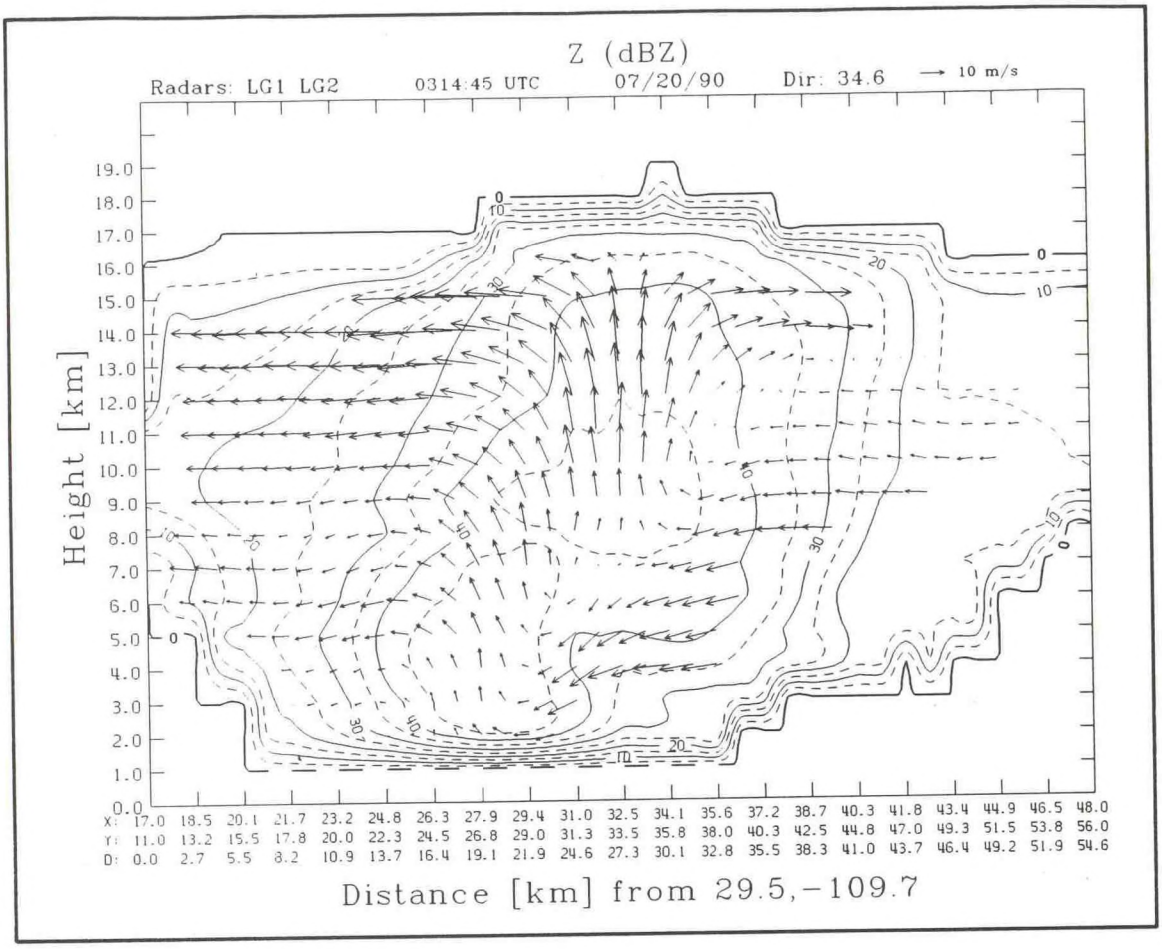

Figure 32. Southwest-northeast vertical cross section through an intense convective cell observed over the high terrain of Mexico on 20 July 1990. Contours of radar reflectivity alternate between solid and dashed lines for each 5-dBZ contour interval. Ground-relative wind vectors are derived using FAST.

difference between the two periods was that low-level moist air was being transported northward from Mexico and the Gulf of California into the state during the high-lightning period. During the low-lightning period, the low-level flow was northerly and quite dry. Otherwise, the remainder of the atmosphere was approximately the same for both periods. Future lightning studies using longer-period lightning, rawinsonde, and satellite archives are planned. A primary emphasis will be to isolate periods of high lightning frequency and thus determine characteristic flow patterns to learn more about the seeds and modes of Arizona thunderstorm development.

NSSL continues research with infrared satellite imagery for diagnosing the role of convective storms and systems in defining regional climate. Hourly infrared satellite imagery is composited to define cloud-top temperature frequencies over periods of days to entire seasons. The composite images are constructed using hourly images with an effective pixel resolution of 7 by 7 km over 61 different temperature thresholds. Initially, the composites were used to assess thunderstorm activity over Mexico in comparison to traditional climate depictions. The work has been expanded to examine the frequency and horizontal coverage of thunderstorm activity during different

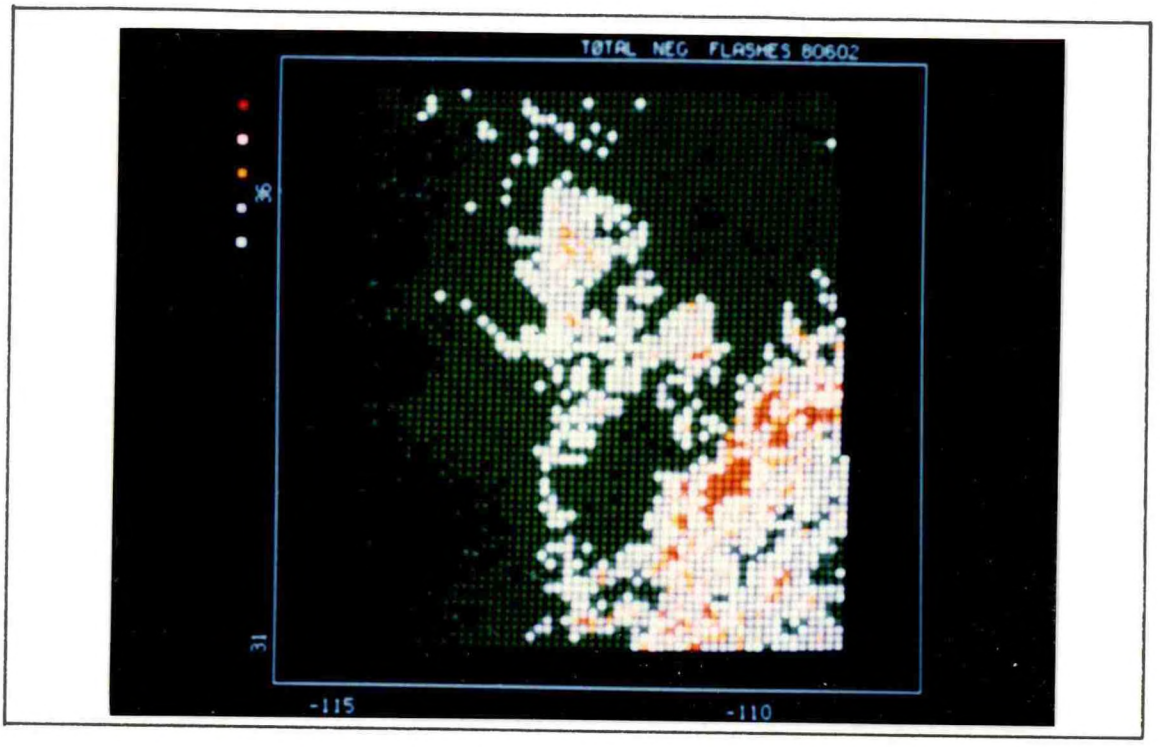

Figure 33. Frequency of lightning flashes across Arizona from 19 July to 24 July 1990, during SWAMP.

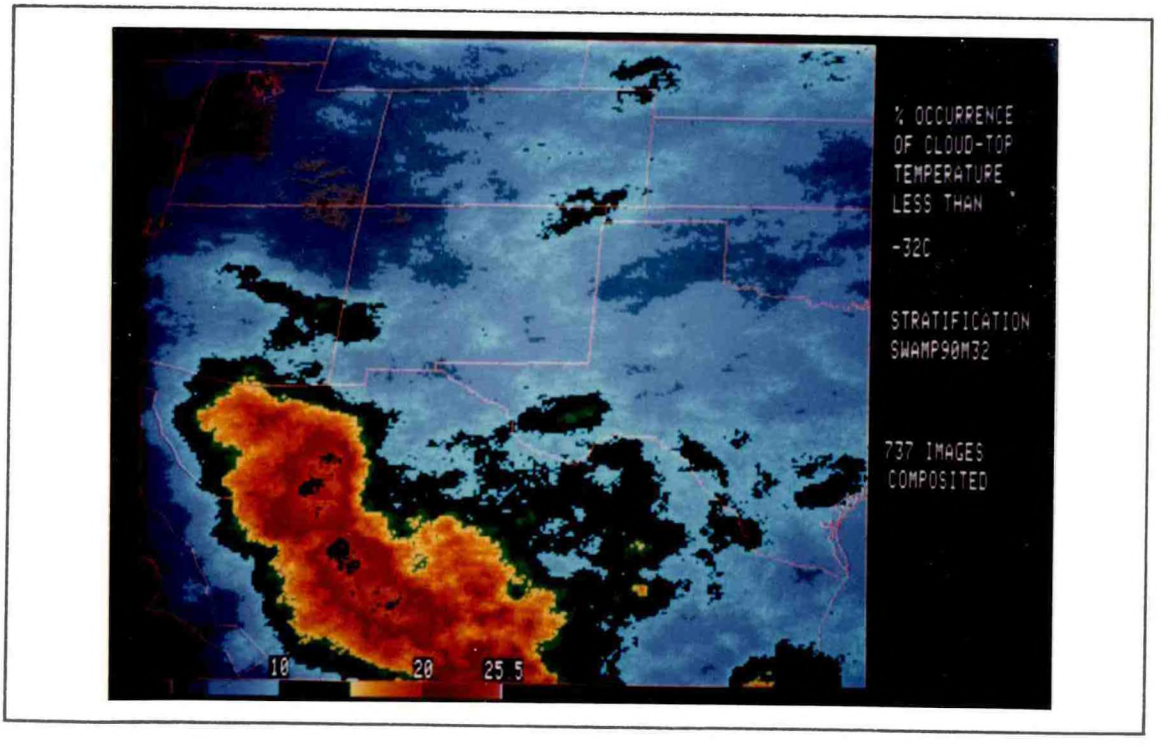

Figure 34. Percent occurrence of cloud-top temperatures less than -32 °C composited from 737 infrared satellite images obtained during SWAMP.

synoptic flows over Florida and over the southwestern United States and Mexico (Figure 34). The composite fields have been used in simple techniques for the estimation of rainfall over the western United States. Preliminary results show that application of frequency composites in the estimation of rainfall on climatological time scales has some skill. An expansion of the satellite climatologies during the next year will include the use of the 6.7 μm water-vapor channel and intercomparisons with SSM/I data collected over Mexico.

Improvement of Radiosonde and M-CLASS Performance

Building on NSSL's pioneering work in mobile ballooning, a test plan was developed and carried out to assess the operation of sondes used with the NSSL M-CLASS in the following four categories: clear air; near storms but outside storm clouds; stratiform precipitation regions; and convective storms. To quantify performance in storms, electric field meters were flown to measure values of the electric field at which the sondes can malfunction. NSSL's new antenna design and receiver module, which was developed in collaboration with NCAR, improved sonde performance significantly. Thermodynamic data--temperature, pressure, dewpoint--and wind information were obtained nearly all the time in the first three categories. Furthermore, based on the few flights made this year, the meteorological sounding data were gathered more of the time in storms.

Balloon-Borne Instrument Development

Under partial funding from NSF, an electro-optical instrument to measure the charge and size of precipitation particles, along with electric field measurements, was developed, tested, and made initial flights. This instrument was flown into severe storms and MCSs. The data will be used to determine the electrical nature of the storms and MCSs and to provide constraints for models. As part of this effort, enhanced data acquisition capabilities for the NSSL balloon-borne electric field meter are being developed and tested.

Computing Facilities

NSSL's computing capabilities continued to be expanded and improved in FY 1990 (Figure 35). NSSL enhanced its VAX cluster capabilities by adding two 1.2 GB disk drives, boosting total disk storage to 5.8 GB. A new communication package, MultiNET TCP/IP, was installed on the VAX 6310 as were two graphic software packages, IDL and DISPLAY. The data archive capabilities of the VAX clusters at Norman and Boulder will be greatly enhanced with two 8-mm tape subsystems in FY 1991. The MicroVAX-based DARE workstation was installed, and negotiations are continuing so the NSSL workstation can be integrated into the NWS data link.

The SUN system at NSSL was expanded considerably in FY 1990 with the addition of two SPARCstation 1+ systems and a SUN 3/110. The SUN network will be improved in FY 1991 by upgrading the 3/280 to a SUN 4/380, increasing its computing power from 4 to 16 MIPS. Disk storage capacity will be increased with the purchase and installation of a 2.5 GB disk drive. Additional plans for FY 1991 include increasing the memory of the 4/380 from 8MB to 32MB, a 24-bit color board for one of the SPARCstations for enhanced graphics, and possible upgrades to two SPARCstations.

A TCP/IP software package was installed on the Concurrent 3280, allowing it to become a member of the NSSL network. A 9-track high-density tape drive and an 8-mm tape-drive subsystem improved data archiving capabilities on the Concurrent, and a 2.5 GB fixed disk subsystem was procured to improve on-line disk storage capabilities. Equipment to interface the Concurrent to the Cimarron radar was procured and will be installed during FY 1991. The Concurrent will be interfaced to the Cimarron radar to ingest and process the radar data, and then broadcast these data to the SUN systems via the network for further analysis and display.

The PC network continues to grow; approximately 70 PCs currently are networked throughout NSSL. The graphics PC was upgraded to a 33 MHz 386-based

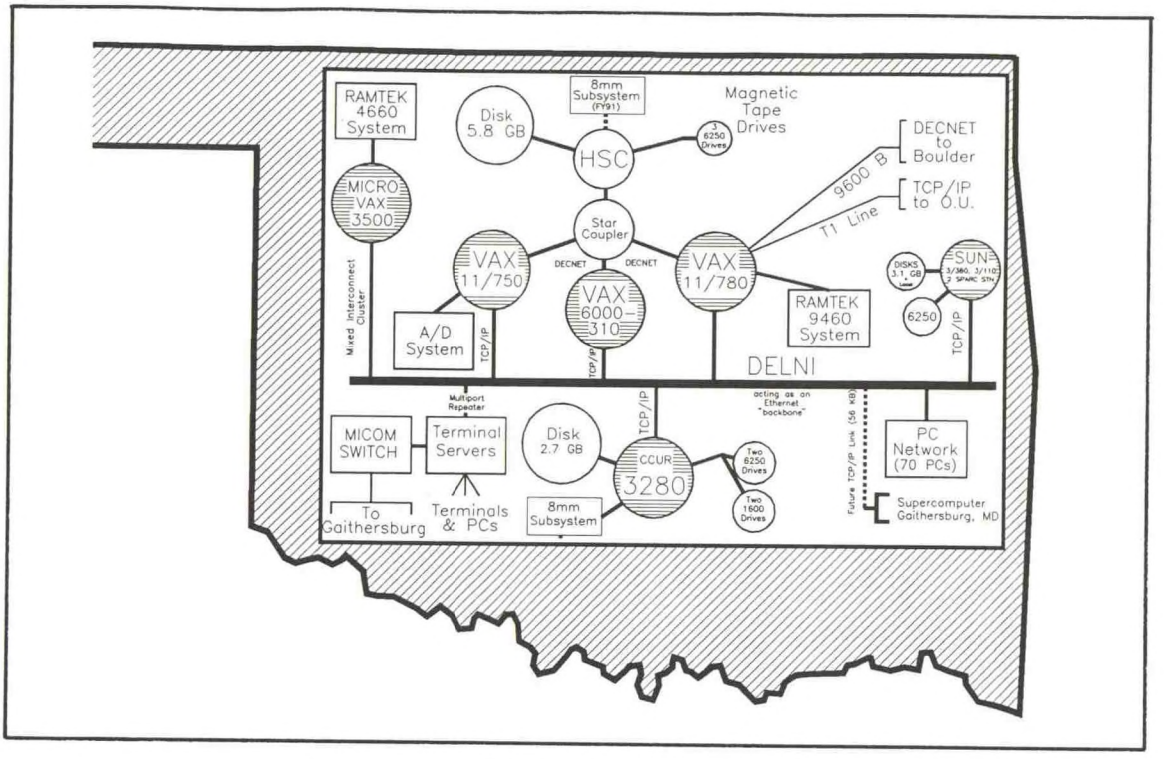

Figure 35. Configuration of NSSL computing facility in Norman.

computer, and a Montage 35-mm camera system was installed to produce slides and prints of PC-derived images. The Laboratory's network was improved with the upgrade of a Xyplex terminal server and the purchase of a network analyzer. Both terminal servers, the Xyplex and VISTA, were expanded to allow dual protocol, permitting personnel to perform TELNET communication from asynchronous terminals. Improvements to the network in FY 1991 will include segmentation of the network using bridges and/or routers. This will isolate various segments of the network and decrease overall network traffic. Upgrades to the NIST link will be made in anticipation of the new supercomputer installation, and plans are under way to fund a microwave-based Ethernet link between the University of Oklahoma and NSSL.

A 65 KVA UPS was installed and is supplying uninterrupted power to the computer and workstation rooms and the SSD office area. The security system was upgraded with card access to the technicians' area and media room. The Laboratory was transferred to the FTS2000 telephone service in June.

Cimarron Radar Upgrades

The Cimarron Doppler radar upgrade neared completion in FY 1990, and operations are being planned for mid-1991. The FAA-funded upgrades to the radar were made to improve its data acquisition speed and polarization measurement performance. Outdated processing equipment was removed and the new programmable signal processor (SP20) and host computers (FORCE) were installed and are undergoing extensive testing. The microwave link between Norman and Cimarron, installed last year, has been tested and shown to be functional. The upgrade will be completed in FY 1991. Remote control capabilities are being developed that will allow remote operations of the radar from Norman. A major advance in data archive capabilities will result from

the installation of an 8-mm tape subsystem that will provide 2.5 GB of storage per tape cassette, or approximately 50 times the current storage media. The Norman processor will be interfaced to the Concurrent 3280 through the VME-bus for algorithm processing and real-time evaluation.

Mobile Laboratories and M-CLASS

FY 1990 saw the activation of a new NSSL mobile laboratory, NSSL2. It was designed for mobile ballooning and was equipped with a new Compaq 386 M-CLASS system and enough on-board helium for approximately 12 flights. NSSL2 was also equipped with a rooftop air conditioner and heater, power generator, equipment racks, extensive communication gear, and an intercom system that allows on-line voice and radio communications throughout the mobile laboratory. Two new types of communication equipment were tested on NSSL2: an 800 MHz radio and a satellite uplink system. The 800 MHz radio provides short-range to intermediate-range voice communication between vehicles, along with cellular phone communications. The satellite uplink provides medium bandwidth, near real-time communication from any location within the United States. The satellite uplink also provides positioning information of the mobile laboratory, allowing the base station to identify its location to within 1000 feet. Instrumentation for temperature, humidity, and wind speed was installed and interfaced with a 386-based computer. Compass heading and speedometer data were also incorporated into the computer so that winds could be determined while the laboratory was mobile. NSSL1's M-CLASS was upgraded with a new Compaq 386, and instrumented with meteorological sensors.

Both mobile laboratories were deployed to field experiments during FY 1990. NSSL1 performed fixed-base ballooning support for the TDWR test in Orlando, Florida. NSSL2 provided mobile ballooning support for SWAMP in Phoenix (Figure 36). Both vehicles are scheduled to support the COPS-91 experiment next year. In FY 1991, both vehicles will have the satellite system installed and the 800-MHz radio will be added to NSSL1. Two additional CLASSs were also purchased by NSSL in FY 1990. The NSSL now has two mobile CLASSs, one fixed-base system and one configured as a dropsonde unit.

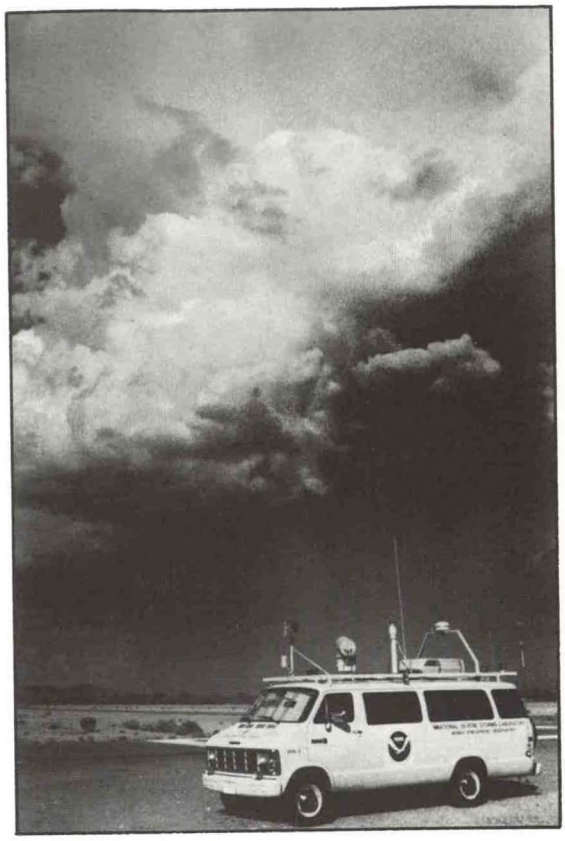

Figure 36. NSSL2 during SWAMP in the Phoenix area. Photograph by Sherman Fredrickson.

Lightning Location and Error Analysis Methods

The performance of the Passi-López algorithm for recovery of site-specific errors in DF networks was tested under controlled, simulated conditions. The simulations showed that the algorithm works well for networks of four or more DFs, but that networks of three DFs have some inherent shortcomings for the recovery of site errors from historical data sets. These limitations have been shown to be fundamental to the

general problem of site error estimation using azimuth data. Several ways to resolve these basic complications were tested with simulations. From these it appeared that the problems would be ameliorated if networks of at least four DFs were used. When there were at least four, the use of an initial guess of the site error curve based on the closest-two-DFs solution, not on an optimized solution involving all DFs, provided faster convergence of the iterative algorithm. If the antennas were perfectly aligned with true north, the site errors could also be recovered reasonably well in the case of three-DF networks. The higher the DF gain, so that more DFs detected each flash, the more accurately the algorithm recovered the site errors. The algorithm was applied to data sets from Florida, Colorado, and Oklahoma. Data from more than half the years from Florida have been analyzed, and final flash positions have been calculated. The data are being gridded into 10 by 10 km boxes for each hour, in preparation for the development of a lightning climatology for central Florida based on 8 years' observations.

Weak Positive CG Flashes in Northeastern Colorado

Frequency distributions of the peak magnetic fields of positive and negative CG flashes have been studied with lightning data from northeastern Colorado. There appear to be fundamental differences in the magnetic field signal strength distributions of the two polarities. Both appear to have the same median signal strengths, but the positive sample has a larger proportion of very small signals. The positive sample lacks the large percentage of signals of intermediate values that are frequent in the negative group. The two distributions are more similar in their relative frequency of large values, but the positive sample, although about 15 times smaller in numbers, contains the largest values of peak signal.

The very weak positive flashes are lost to the medium-to-high gain Colorado detection system very quickly with increasing range. The detected signals are thus the stronger ones, and the averages for samples of positive flashes distant from the DFs appear higher than do those for similar samples of negative flashes. When only flashes very close (20-60 km) to the DFs are considered (Figure 37), the two distributions have almost identical medians.

The large percentage of weak positive signals detected close to the DFs has not been previously emphasized. It has been suggested that the signals come from intracloud discharges and so are improperly classified as coming from CG flashes. The evidence in hand, however, points to their being real positive, albeit weak, CG flashes. Whether they are real positive ground flashes or not, it is important to be aware of their presence in data from magnetic DF networks, especially when data from medium-to-high gain and low-gain networks are used. Thus, for example, similar large percentages of weak positives have been reported in the new low-gain network at Kennedy Space Center in Florida.

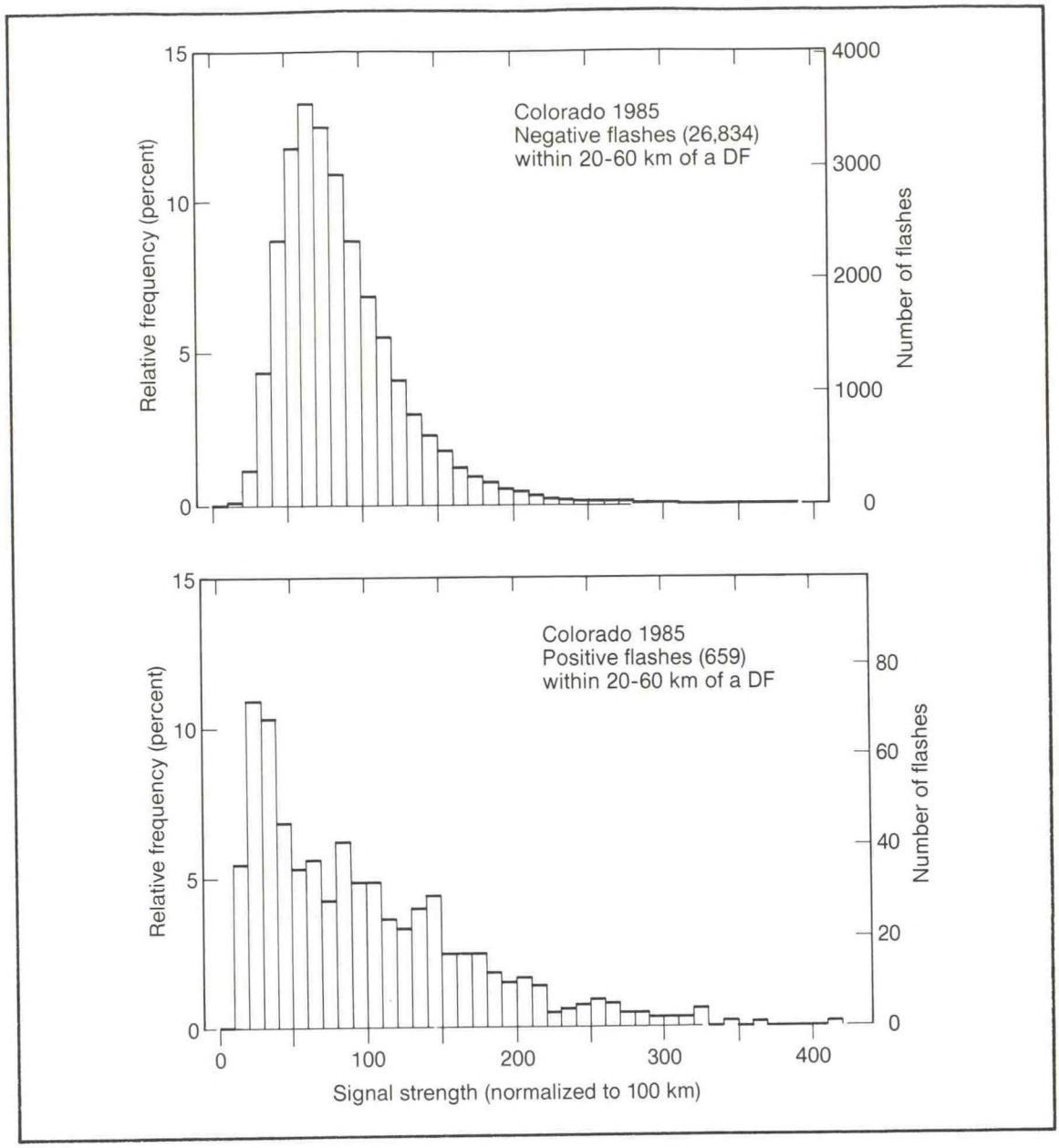

Figure 37. Normalized peak signal strengths for negative (top) and positive (bottom) flashes within 20-60 km of a DF.

NSSL STAFF FY 1990

Office of the Director

Robert A. Maddox	Director
Doviak, Richard J.	Electrical Engineer
McCollum, Darren	CIMMS Student
Maki, Masayuki	Visitor - Japan
Meacham, Mary E.	Librarian
Walton, Joy L.	Secretary
Winston, Karen	Meteorological Aid

Administration

L. Don Howard	Administrative Officer
Gregory, Patricia R.	Purchasing Agent
Kelly, Stephanie K.	Administrative Aid

Doppler Radar and Remote Sensing Group

Dusan S. Zrnic´	Manager
Antolik, Mark S.	CIMMS Student
Brandes, Edward A.	Meteorologist
Brooks, Harold	NRC Post-Doctorate
Brown, Rodger A.	Meteorologist
Conway, John W.	CIMMS Student
Davies-Jones, Robert P.	Meteorologist
Doswell, Charles A. III	Meteorologist
Gal-Chen, Josefa	CIMMS Programmer
Gold, David	Meteorological Aid
Hornecker, Melissa	Meteorological Aid
Lynn, Kelly S.	Secretary
Moritz, Michael L.	Meteorological Aid
Spaeth, Daniel	Meteorological Technician

Forecast Applications Research Group

Donald W. Burgess	Manager
Eilts, Michael D.	Meteorologist
Gilmore, Matthew	Meteorological Aid
Hermes, Laurie G.	Meteorologist
Hondl, Kurt D.	CIMMS Associate
Jincai, Ding	Visitor - Peoples Republic of China
Johnson, James T., Jr.	CIMMS Student
Livingston, Cindy W.	Secretary
Mitchell, Dewayne	Physical Science Aid
Morris, Dale	Physical Science Aid
Smith, Travis M.	Meteorological Aid
Stumpf, Gregory J.	CIMMS Associate
Thomas, Kevin W.	CIMMS Senior Program Analyst
Vasiloff, Steven V.	Meteorologist
Witt, Arthur	Meteorologist
Wood, Vincent T.	Meteorologist

Mesoscale Research Division (Boulder)

David P. Jorgensen	Manager (Acting)
Augustine, John A.	Meteorologist
Bartels, Diana L.	Meteorologist
Blanchard, David O.	Meteorologist
Caracena, Fernando	Physicist
Chandler, Sandra J.	Secretary
Daugherty, John R.	Physical Scientist
Douglas, Michael	CIRES Research Associate
Holle, Ronald L.	Meteorologist
Howard, Kenneth W.	Meteorologist
Hueftle, Robert A.	Computer Programmer
Li, Lin	CIRES Research Assistant
López, Raúl E.	Meteorologist
Matejka, Thomas	Meteorologist
Meitín, José G., Jr.	Meteorologist
Ortiz, Robert	Meteorologist
Schuur, Terry	CIRES Associate
Smull, Bradley F.	Meteorologist
Tyalha, Lori J.	Physical Scientist
Watson, Andrew I.	Meteorologist

Meteorological Research Group

John M. Lewis	Manager
Bao, Jian-Wen	Student - Peoples Republic of China
Bickford, Dan	Graduate Student
Hane, Carl E.	Meteorologist
Kogan, Yefim L.	CIMMS Research Scientist
Li, Yong	Student - Peoples Republic of China
Liu, Qingfu	CIMMS Student
Livingston, Cindy W.	Secretary
Martin, William J.	CIMMS Associate
Mechem, David B.	Meteorological Aid
Rabin, Robert M.	Meteorologist
Smith, Walter	NRC Post-Doctorate
Stensrud, David J.	Meteorologist
Thompson, Richard	CIMMS Student
Xu, Qin	CIMMS Research Scientist
Ziegler, Conrad L.	Meteorologist

Scientific Support Division

Douglas E. Forsyth	Asst. Director/Manager
Devericks, Lawrence S.	Clerk-Typist
Doctor, Jo Retta K.	Secretary
Fredrickson, Sherman E.	Meteorologist

Computing and Data Management

Jain, Michael H.
Supervisory Meteorologist
Green, Clifford L.
CIMMS Support Programmer
Kelleher, Kevin E.
CIMMS Manager, Scientific Computing
Liang, Daniel — CIMMS Student
Ross, Catherine L. — Computer Assistant
Skaggs, Gary A. — Meteorological Technician
Wardius, Gerald J.
Meteorological Technician

Engineering

Carter, John K. — Electronics Engineer
Zahrai, F. Allen — Electronics Engineer

Technical Support

Anderson, Glen H., Jr.
Lead Electronics Technician
Griffin, Lawrence P. — Electronics Technician
McGowen, James W. — Electronics Technician
Nealson, Dennis E. — Electronics Technician
Schmidt, J. Michael — Electronics Technician
Wahkinney, Richard J.
Student Trainee Electronics Technician

Technical Field Support

Showell, Lester C.
Supervisory Meteorological Technician
George, Charlie — Meteorological Aid
Crisp, Charlie A. — Meteorological Technician
Keller, David — CIMMS Associate
Kimpel, Joan — CIMMS Graphic Artist
Porter, Christopher
Meteorological Technician
Wheeler, Douglas R. — Meteorological Aid

Contract Staff - The Software & Hardware Group, Inc.

Jeffrey Pitts — Computer Operator
Steve Million — Computer Operator
Sarah Sanger — Systems Analyst

Storm Electricity and Cloud Physics Group

W. David Rust — Manager
Bateman, Monte — Physics Student
Crider, Donna — Meteorological Aid
Douglass, Brenda L. — CIMMS Student
Harbour, Christine M. — CIMMS Student
Hunter, Steven M. — CIMMS Associate
Lee, Lin — CIMMS Student
MacGorman, Donald R. — Physicist
Mazur, Vladislav — Physicist
McCourry, Stanton A. — Engineering Aid
Morgenstern, Carol — USAF
Rhoden, Gene — Meteorological Aid
Rhue, Douglas T. — Computer Programmer
Shepherd, Tommy R. — CIMMS Student
Younkins, Mary L. — Secretary

FY 1990 PUBLICATION LIST

Antolik, M.A., and C.A. Doswell III, 1989: On the contribution to model-forecast vertical motion from quasi-geostrophic processes. Preprints, 12th Conference on Weather Analysis and Forecasting, October 2-6, Monterey, CA, Amer. Meteor. Soc., Boston, 312-318.

Augustine, J.A., E. Tollerud, and B. Jamison, 1989: Distributions and other general characteristics of mesoscale convective systems during 1986 as determined from GOES infrared imagery. Preprints, 12th Conference on Weather Analysis and Forecasting, October 2-6, Monterey, CA, Amer. Meteor. Soc., Boston, 437-442.

Balakrishnan, N., and D.S. Zrnic´, 1990: Estimation of rain and hail rates in mixed-phase precipitation. *J. Atmos. Sci., 47,* 565-583.

Balakrishnan, N., and D.S. Zrnic´, 1990: Use of polarization to characterize precipitation and discriminate large hail. *J. Atmos. Sci., 47,* 1525-1540.

Bartels, D.L., and R.A. Maddox, 1989: A satellite based climatology of mid-level cyclonic vortices generated by mesoscale convective complexes. Preprints, 12th Conference on Weather Analysis and Forecasting, October 2-6, Monterey, CA, Amer. Meteor. Soc., Boston, 87-92.

Blanchard, D.O., 1990: Mesoscale convective patterns of the southern High Plains. *Bull. Amer. Meteor. Soc., 71,* 994-1005.

Bluestein, H.B., E.W. McCaul, Jr., G.P. Byrd, R.L. Walko, and R.P. Davies-Jones, 1990: An observational study of splitting convective clouds. *Mon. Wea. Rev., 118,* 1359-1370.

Brandes, E.A., 1990: Evolution and structure of the 6-7 May 1985 mesoscale convective system and associated vortex. *Mon. Wea. Rev., 118,* 109-129.

Burgess, D.W., and L.R. Lemon, 1990: Severe thunderstorm detection by radar. In *Radar in Meteorology: Battan Memorial and 40th Anniversary Radar Meteorology Conference,* D. Atlas (ed.), Amer. Meteor. Soc., Boston, 619-647.

Caracena, F., 1989: Low pass filter response characteristics of analytic approximations by weighted sums for single pass, multipass, and optimal schemes. Preprints, 11th Conference on Probability and Statistics in Atmospheric Sciences, October 2-6, Monterey, CA, Amer. Meteor. Soc., Boston, 20-25.

Caracena, F., and A. Marroquin, 1990: The use of a gridless analysis scheme in complex, diagnostic calculations. Extended Abstracts, WMO International Symposium on Assimilation of Observations in Meteorology and Oceanography, July 9-13, Clermont-Ferrand, France, World Meteorological Organization, Geneva, Switzerland, 566-571.

Carbone, R., B. Foote, M. Moncrief, T. Gal-Chen, W. Cotton, M. Hjelmfelt, F. Roux, G. Heymsfield, and E. Brandes, 1990: Convective dynamics: Panel report. In *Radar in Meteorology: Battan Memorial and 40th Anniversary Radar Meteorology Conference,* D. Atlas (ed.), Amer. Meteor. Soc., Boston, 391-400.

Carpenter, R.L., K.K. Droegemeier, P.R. Woodward, and C.E. Hane, 1990: Application of the piecewise parabolic method to meteorological modeling. *Mon. Wea. Rev., 118,* 586-612.

Conway, J.W., and D.S. Zrnic´, 1990: The differential reflectivity column: Its importance as embryo source and hailgrowth regions. Preprints, 1990 Conference on Cloud Physics, July 23-27, San Francisco, CA, Amer. Meteor. Soc., Boston, 432-436.

Doswell, C.A. III, 1990: Comments on 'On the need for augmentation in automated surface observations.' *National Wea. Digest, 15,* 29-30.

Doswell, C.A. III, 1989: Comments on 'Vertical motion evaluation of a Colorado snowstorm from a synoptician's perspective.' *Wea. Forecasting, 4,* 568-570.

Doswell, C.A. III, 1990: On the use of hodographs: Vertical wind profile information applied to forecasting severe thunderstorms (2nd ed.). NOAA/NWS/SRH, Scientific Services Division, Fort Worth, TX, and NOAA/ERL, National Severe Storms Laboratory, Norman, OK, 37 pp.

Douglas, M.W., M.A. Shapiro, L.S. Fedor, and L. Saukkonen, 1990: Research aircraft observations of a polar low at the East-Greenland ice-edge. Extended Abstracts, 4th Conference on Mesoscale Processes, June 25-29, Boulder, CO, Amer. Meteor. Soc., Boston, 22-23.

Doviak, R.J., K.W. Thomas, and D.R. Christie, 1989: The wavefront shape, position, and evolution of a great solitary wave of translation. *IEEE Trans. Geosci. Remote Sensing, 27,* 658-665.

Eilts, M.D., and S.D. Smith, 1990: Efficient dealiasing of Doppler velocities using local environment constraints. *J. Atmos. Oceanic Tech., 7,* 118-128.

Forsyth, D.E., D.W. Burgess, C.A. Doswell III, M.H. Jain, L.E. Mooney, R.M. Rabin, and W.D. Rust, 1990: DOPLIGHT '87 Project Summary. NOAA TM ERL NSSL-101 (PB90-253584), 83 pp.

Fulton, R., D.S. Zrnic´, and R.J. Doviak, 1990: Initiation of a solitary wave family in the demise of a nocturnal thunderstorm density current. *J. Atmos. Sci., 47,* 319-337.

Hane, C.E., 1990: Retrieval of dynamic variables in convective cloud systems observed by Doppler radar. *Atmos. Res., 25,* 217-234.

Holle, R.L., R.E. López, and A.I. Watson, 1990: Cloud-to-ground lightning detection using direction-finder networks: Recent advances and applications. *Bull. World Meteor. Org., 39,* 177-179.

Houze, R.A., B.F. Smull, and P. Dodge, 1990: Mesoscale organization of springtime rainstorms in Oklahoma. *Mon. Wea. Rev., 118,* 613-654.

Johnson, R., S. Chen, G. Stumpf, and D. Bartels, 1990: The vertical structure of a midtropospheric vortex within the stratiform region of a mesoscale convective system. Extended Abstracts, 4th Conference on Mesoscale Processes, June 25-29, Boulder, CO, Amer. Meteor. Soc., Boston, 216-217.

Jorgensen, D.P., and R. Meneghini, 1989: Airborne/spaceborne radar: Panel report. In *Radar in Meteorology: Battan Memorial and 40th Anniversary Radar Meteorology Conference,* D. Atlas (ed.), Amer. Meteor. Soc., Boston, 315-322.

Lee, J.T., and K. Thomas, 1990: Turbulence spectral widths view angle independence as observed by Doppler radar. Final Report DOT/FAA/SA-89/2 to Federal Aviation Administration. Available through NTIS, Springfield, VA 22161, 47 pp.

LeMone, M.A., and D.P. Jorgensen, 1990: Momentum generation and redistribution in a TAMEX convective band. Preprints, Workshop on TAMEX Scientific Results, September 24-26, Boulder, CO, National Center for Atmospheric Research, Boulder, 42-47.

LeMone, M.A., J.C. Fankhauser, and T. Matejka, 1990: Momentum generation and redistribution in convective bands: What have we learned? Extended Abstracts, 4th Conference on Mesoscale Processes, June 25-29, Boulder, CO, Amer. Meteor. Soc., Boston, 198-199.

Lewis, J., C. Hayden, and J. Derber, 1989: A method for combining radiances and wind shear to define the temperature structure of the atmosphere. *Bull. Amer. Meteor. Soc., 117,* 1193-1207.

Matejka, T., and M.A. LeMone, 1990: The generation and redistribution of momentum in a squall line. Extended Abstracts, 4th Conference on Mesoscale Processes, June 25-29, Boulder, CO, Amer. Meteor. Soc., Boston, 196-197.

Matejka, T., and C.L. Ziegler, 1990: The effect of hydrometeor evolution on dynamical processes in the stratiform region of a mesoscale convective system. Preprints, 1990 Conference on Cloud Physics, July 23-27, San Francisco, CA, Amer. Meteor. Soc., Boston, 679-682.

Mazur, V., and B.D. Fisher, 1990: Cloud-to-ground strikes to the NASA F-106 airplane. *J. Aircraft, 27,* 466-468.

Mazur, V., B.D. Fisher, and P.W. Brown, 1990: Multistroke cloud-to-ground strike to the NASA F-106B airplane. *J. Geophys. Res., 9,* 5471-5484.

Parsons, D.B., B.F. Smull, and D.K. Lilly, 1989: Mesoscale organization and processes: Panel report. In *Radar in Meteorology: Battan Memorial and 40th Anniversary Radar Meteorology Conference,* D. Atlas (ed.), Amer. Meteor. Soc., Boston, 461-476.

Rabin, R.M., 1989: Capabilities of measuring cloud variability from satellites. Proceedings, Workshop on Mechanisms for Tropospheric Effects of Solar Variability and the Quasi-Biennial Oscillation, June 20-21, Boulder, CO, National Center for Atmospheric Research, Boulder, 42-74.

Rabin, R.M., and R.J. Doviak, 1989: Meteorological and astronomical influences on radar reflectivity in the convective boundary layer. *J. Appl. Meteor., 28,* 1226-1235.

Rabin, R.M., S.J. Stadler, P. Wetzel, D.J. Stensrud, and M. Gregory, 1990: Observed effects of landscape variability on convective clouds. *Bull. Amer. Meteor. Soc., 71,* 272-280.

Ray, P.S., C.L. Ziegler, and S.L. Lang, 1990: Retrieval of microphysical variables in New Mexican mountain thunderstorms from Doppler radar data. Preprints, 1990 Conference on Cloud Physics, July 23-27, San Francisco, CA, Amer. Meteor. Soc., Boston, 437-442.

Rust, W.D., R.P. Davies-Jones, D.W. Burgess, R.A. Maddox, L.C. Showell, T.C. Marshall, and D.K. Lauritsen, 1990: Testing a mobile version of a cross-chain atmospheric sounding system (M-CLASS). *Bull. Amer. Meteor. Soc., 71,* 173-180.

Rutledge, S.A., C. Lu, and D.R. MacGorman, 1990: Positive cloud-to-ground lightning in mesoscale convective systems. *J. Atmos. Sci., 47,* 2085-2100.

Smull, B.F., and D.P. Jorgensen, 1990: Pressure and buoyancy perturbations near an intense wake low in a midlatitude mesoscale convective system. Extended Abstracts, 4th Conference on Mesoscale Processes, June 25-29, Boulder, CO, Amer. Meteor. Soc., Boston, 214-215.

Stumpf, G.J., 1990: The gust front detection algorithm for the terminal Doppler weather radar: Impact of NEXRAD scan strategies; detecting non-gust front phenomena. Preprints, 10th Annual International Geosciences & Remote Sensing Symposium, May 20-24, College Park, MD, 743-746.

Szoke, E.J., and J.A. Augustine, 1990: An examination of the mean flow and thermodynamic characteristics of a mesoscale flow feature: The Denver cyclone. Extended Abstracts, 4th Conference on Mesoscale Processes, June 25-29, Boulder, CO, Amer. Meteor. Soc., Boston, J17-J18.

Tollerud, E., J. Brown, and D.L. Bartels, 1989: Structure of an MCS-induced mesoscale vortex as revealed by VHF profiler, Doppler radar, and satellite observations. Preprints, 12th Conference on Weather Analysis and Forecasting, October 2-6, Monterey, CA, Amer. Meteor. Soc., Boston, 81-86.

Williams, E., V. Mazur, and S. Geotis, 1990: Lightning investigation with radar. In *Radar in Meteorology: Battan Memorial and 40th Anniversary Radar Meteorology Conference*, D. Atlas (ed.), Amer. Meteor. Soc., Boston, 143-150.

Zrnic´, D.S., 1990: Signal processing: Panel report. In *Radar in Meteorology: Battan Memorial and 40th Anniversary Radar Meteorology Conference*, D. Atlas (ed.), Amer. Meteor. Soc., Boston, 230-234.

Zrnic´, D.S. and Z. Banjanin, 1989: Ground clutter filters for staggered pulse trains. Final Report DOT/FAA/SA-89/2, Federal Aviation Administration, Washington, DC, 57 pp.

MAJOR SEMINARS AT NSSL–at Norman (N) and Boulder (B)

23 October 1989	Dr. R. Schlesinger, University of Wisconsin, Madison, WI, presented "Feedback of a convective storm to the near environment as diagnosed from three-dimensional cloud model output." (N)
25 October 1989	Dr. T. Matejka, NSSL, ERL, presented "The generation and redistribution of momentum in a squall line." (N)
4 January 1990	Dr. M. Demaria, Atlantic Oceanographic and Meteorological Laboratory, ERL, Miami, FL, presented "An overview of hurricane track prediction." (N)
16 February 1990	Dr. H. Brooks, University of Illinois, Urbana, IL, presented "Effects of low-level hodograph curvature on numerically-modeled thunderstorms." (N)
28 February 1990	Dr. N. Junker, National Meteorological Center, NWS, Camp Springs, MD, presented "Performance of the NMC operational models in predicting precipitation." (N)
4 April 1990	Dr. T. Matejka, NSSL, ERL, Boulder, CO, presented "New ideas in velocity-azimuth display analysis of single Doppler radar data: EVAD and CEVAD." (N)
9 May 1990	Dr. D. P. Jorgensen, NSSL, ERL, Boulder, CO, presented "Airborne Doppler editing and analysis tools at MRD." (N)
13 June 1990	Dr. J. Schmidt, Colorado State University, Fort Collins, CO, presented "A numerical and observational investigation of long-lived severe surface wind events: The 2 August 1981 CCOPE and 12-13 May 1985 PRE-STORM derechos." (N)
6 July 1990	Ms. D. Jacob, GKSS Forschungszentrun, Geesthacht, Federal Republic of Germany, presented "A simulated sea-breeze circulation system in northern Germany." (N)
20 July 1990	Dr. R. Hodur, Naval Oceanographic and Atmospheric Research Laboratory, Monterey, CA, presented "Numerical modeling at NOARL-West." (N)

MEETINGS HOSTED BY NSSL

12 February 1990	NOAA Mesoscale Planning Team in Norman.
13-14 February 1990	NSSL Program Review in Norman.
3 April 1990	COPS-91 Planning Meeting in Norman.
4 April 1990	Subcommittee on Atmospheric Research in Norman. Members include Dr. E. Bierly and Mrs. J. Jordan of National Science Foundation; Col. T. Cress, Department of Defense; Dr. J. Almazan, Office of Federal Coordinator for Meteorological Services, NOAA; Mr. L. Moore, U.S. Bureau of Reclamation, Department of Interior; Dr. N. Strommen, Department of Agriculture; Dr. F. Einaudi, NASA/Goddard; Mr. D. Tuttle, FAA, Department of Transportation; and Mr. C. Goff, FAA, Department of Transportation.
12 April 1990	National Weather Service Modernization Committee, National Research Council, Commission on Engineering and Technical Systems in Norman. Committee consisted of Dr. C. Hosler, Chairman; Mr. P. Leavitt, Mr. L. Snellman, Dr. D. Veal, Mr. A. Zygielbaum, Mr. D. Johnson, Mr. L. Boezi, Mr. N. Scheller, and Dr. D. Sargeant.
22 June 1990	Portion of Oklahoma Summer Scholars Program (hosted by Department of History of Science, University of Oklahoma) in Norman.
26 June 1990	Portion of Summer Institute for Earth Science Teachers (hosted by School of Meteorology, University of Oklahoma) in Norman.
16, 20 August 1990	Delegation from China to discuss LLP systems and related lightning research in Boulder (16th) and Norman (20th).

VISITORS TO NSSL – at Norman (N) and Boulder (B)

F. Abatemarco	*Popular Science*, New York, NY (B)
M. Adams	Air Weather Service, Patrick Air Force Base, FL (B)
H. Arellano	Secretaria Governacion, Mexico (N)
N. Arias	Civil Aviation Agency, Bogota, Columbia (B)
T. Bakke	Norwegian Television (N)
W. Bauman	Air Weather Service, Patrick Air Force Base, FL (B)
H. Bluestein	University of Oklahoma, Norman, OK (B)
W. Boerner	University of Illinois, Chicago, IL (N)
W. Bohan	Climatological Consulting Corporation, Park Ridge, IL (B)
W. Bonner	COMET, Boulder, CO (N)
M. Brook	New Mexico Institute of Mining & Technology, Socorro, NM (N)
R. Brook	Bureau of Meteorology, Melbourne, Australia (B)
H. Brooks	University of Illinois, Champaign-Urbana, IL (N)
J. Carvajal	Secretaria Governacion, Mexico (N)
G. Chao	Institute of Space Physics, Beijing, China (B, N)
W. Chiang	Central Weather Bureau, Taipei, Taiwan (N)
W. Chuanzhu	Great Wall Industry Corporation, China (B, N)
V. Cooray	University of Uppsala, Sweden (N)
C. Cricenti	3350th Technical Training, Rantoul, IL (N)
J. Culbert	Lincoln Laboratories, Lexington, MA (N)
O. Cylke	Association of Big Eight Universities (N)
M. DeMaria	Atlantic Oceanographic & Meteorological Lab., Miami, FL (N)
V. Dronov	Main Geophysical Observatory, Leningrad, USSR (B)
K. Erdman	MASC Real Property, Boulder, CO (N)
J. Evans	Lincoln Laboratories, Lexington, MA (N)
J. Fletcher	Director, ERL, Boulder, CO (N)
J. Fritsch	Pennsylvania State University, University Park, PA (N)
L. Fushan	Institute of Space Physics, Beijing, China (B, N)
J. Gamache	Atlantic Oceanographic & Meteorological Lab., Miami, FL (B)
J.-A. García-Miguel	University of Madrid, Madrid, Spain (B)
C. Goff	Federal Aviation Administration, Washington, DC (N)

J. Golden	Nat. Weather Service Headquarters, Silver Spring, MD (B)
K. Groninger	MASC Facilities and Logistics, Boulder, CO (N)
C. Guo	Lanzhou Inst. of Plateau Atmospheric Physics, China (B, N)
E. Hernandez	University of Madrid, Madrid, Spain (B)
R. Hodur	Naval Ocean. & Atmos. Research Lab., Monterey, CA (N)
J. Iracheta	Secretaria Gobernacion, Mexico (N)
D. Jacob	GKSS Forschungszentrum, Geesthacht, Germany (N)
D. Jincai	Shanghai Meteorological Center, Shanghai, China (N)
R. Johns	NWS Nat. Severe Storms Forecast Ctr., Kansas City, MO (N)
J. Jordan	National Science Foundation, Washington, DC (N)
B. Jou	National Taiwan University, Taipei, Taiwan (B)
N. Junker	National Meteorological Center, NWS, Washington, DC (N)
A. Kassar	National Institute of Meteorology, Tunis, Tunisia (N)
Z. Kawasaki	Faculty of Engineering, Osaka University, Japan (N)
P. King	Bureau of Meteorology, Sidney, Australia (N)
D. Klingle-Wilson	Lincoln Laboratories, Lexington, MA (N)
P. Krider	University of Arizona, Tucson, AZ (B)
P. Leftwich	NWS Nat. Severe Storms Forecast Ctr., Kansas City, MO (B)
R. Mahler	Deputy Director, ERL, Boulder, CO (N)
T. Marshall	University of Mississippi, Oxford, MS (N)
B. Merrill	Space Science and Engineering Center, Madison, WI (N)
V. Miller	The Weather Channel, Atlanta, GA (B)
J. Moore	National Center for Atmospheric Research, Boulder, CO (N)
H. Moreno	Secretaria De Comunicationes Y Transportes, Mexico (N)
C. Nappo	Air Resources Laboratory, ERL, Oak Ridge, TN (N)
S. Nelson	National Science Foundation, Washington, DC (N)
J. Nicholson	NASA, Kennedy Space Center, FL (B)
T. Noyes	Lincoln Laboratories, Lexington, MA (N)
S. Olson	Lincoln Laboratories, Lexington, MA (N)
D. Owen	COMET, Boulder, CO (N)
D. Parsons	National Center for Atmospheric Research, Boulder, CO (N)
R. Passi	Inst. for Naval Oceanography, Stennis Space Center, MS (B)
R. Petersen	NWS National Meteorological Center, Washington, DC (N)
D. Phillips	Salt River Project, Phoenix, AZ (N)

X. Qingfu	Lanzhou Inst. of Plateau Atmospheric Physics, China (B, N)
S. Rinard	NWS Southern Region, Ft. Worth, TX (N)
G. Runsheng	Institute of Mesoscale Meteorology, Beijing, China (N)
A. Ryzhkov	Main Geophysical Observatory, Leningrad, USSR (N)
M. Sabones	NWS Forecast Office, Melbourne, FL (B)
R. Sater	ERL Budget Services Office, Boulder, CO (N)
M. Schuler	COMET, Boulder, CO (N)
C. Scott	NWS Forecast Office, Anchorage, Alaska (B)
C. Segura	ERL Budget Services Office, Boulder, CO (N)
R. Serafin	National Center for Atmospheric Research, Boulder, CO (N)
G. Shchukin	Main Geophysical Observatory, Leningrad, USSR (B)
E. Shulgina	Main Geophysical Observatory, Leningrad, USSR (B)
A. Shupyatsky	Central Aerological Laboratory, Leningrad, USSR (N)
T. Strange	Air Weather Service, Patrick Air Force Base, FL (B)
M. Tallman	Chief, Weather Training Division, Rantoul, IL (N)
A. Tunis	National Institute of Meteorology, Tunisia (N)
D. Turnbull	Federal Aviation Administration, Washington, DC (N)
J. Vavrek	Hammond School System, Hammond, IN (B, N)
G. Vickers	Atmospheric Environment Service, Alberta, Canada (N)
A. Vigil	MASC Procurement, Boulder, CO (N)
T. Warner	Pennsylvania State University, University Park, PA (N)
A. Watson	Bureau of Meteorology, Melbourne, Australia (B, N)
J. Weems	Air Weather Service, Patrick Air Force Base, FL (B)
S. Weiss	NWS Nat. Severe Storms Forecast Ctr., Kansas City, MO (N)
J. Welsh	Geophysical Fluid Dynamics Laboratory, Princeton, NJ (B, N)
R. Wheeler	Computer Sciences Raytheon, Patrick Air Force Base, FL (B)
W. Wilson	National Center for Atmospheric Research, Boulder, CO (N)
L. Xicheng	Great Wall Industry Corporation, China (B, N)
C. Xuliang	China Oil and Gas Corporation, China (B, N)
A. Yaglom	Atmospheric Turbulence Laboratory, USSR (N)
Y. Yinghua	China Oil and Gas Corporation, China (B, N)
E. Zipser	Texas A & M University, College Station, TX (N)
J. Zysko	NASA, Kennedy Space Center, FL (B)

☆ U.S. GOVERNMENT PRINTING OFFICE: 1991—575-416/45,095 REGION NO. 8